Review

Cellulose-Based Functional Materials for Sensing

Valeria Gabrielli *[ID] and Marco Frasconi *

Department of Chemical Sciences, University of Padova, Via F. Marzolo 1, 35131 Padova, Italy
* Correspondence: valeria.gabrielli@unipd.it (V.G.); marco.frasconi@unipd.it (M.F.)

Abstract: The growing bioeconomic demand for lightweight materials with combined sustainability, large-scale production, ease in functionalization and competitive mechanical properties has seen the revival of cellulose as a scaffold for several applications. In particular, due to its multifunctional features, cellulose has found application in sensor and biosensor fabrication. Nonetheless, the great variety of cellulose properties and formulations makes the choice of the best suited cellulose-based material for a specific sensing strategy a difficult task. This review offers a critical discussion and guide for the reader towards the understanding of which of the multiple cellulose derivatives and properties can be exploited for the optimal performance of the desired sensing device. We introduce the unique molecular structure, nanoarchitecture and main properties of cellulose and its derivatives. The different functionalization approaches for anchoring receptors on cellulose derivatives and the processing methodologies for fabricating cellulose-based sensors are explored. As far as the use and performance of cellulose-based functional materials in sensors is concerned, we discuss the recent advances of optical and electrochemical sensors and biosensors for biomedical and environmental monitoring.

Keywords: cellulose derivatives; nanocelluloses; cellulose hydrogels; cellulose films; sustainable materials; biosensors; paper-based sensors; optical sensors; electrochemical sensors; immunoassays

1. Introduction

Cellulose is the most abundant, natural and renewable biopolymer obtained from agricultural and forest biomass residues. Indeed, cellulose is an essential part in the plant cell wall, and it plays an important role in maintaining plant stiffness and strength. Given its inherent biocompatibility and chirality, cellulose has found new applications in the immobilization of peptides [1] and proteins [2] (including enzymes [3] and antibodies [4,5]), as well as in the separation of enantiomeric molecules [6,7]. Additionally, given the cellulose strength and reinforcing ability, it has been frequently used alone or as composite with synthetic polymers and biopolymers as a support matrix for several applications, including their incorporation in sensing and biosensing devices [8–11].

The fabrication of physical and chemical sensors has commonly witnessed the use of plastic, ceramics, glass and other non-renewable materials. Nonetheless, sensibilization about environmental pollution calls for the implementation of more sustainable materials for sensor development [12]. In this context, cellulose has been reported as an inexhaustible, renewable material and the highest hallmark for green materials. In addition to its biosustainability, cellulose presents different scales of arrangements and ease on functionalization and formulation, which translates into its applicability in field spanning from electronic devices to photonic films and biosensors. For example, cellulose has been used as a platform for immune essays and diagnostic, either as a scaffold for the linking antibodies, or as a support matrix alone or in combination with other polymers [13]. In addition, cellulose membranes have been used for the fabrication of fluorescent sensors for the monitoring of a variety of analytes in different environments. For these reasons, there is a growing trend in the use of cellulose and cellulose derivatives as a substitute of petroleum-based polymers (e.g., polyethylene, PET and PVC), metals or glass for sensors fabrication [14].

This review addresses the topic of cellulose and its derivatives as functional materials in the fabrication of sensors and biosensors. We briefly highlight the different types of celluloses and their properties, emphasizing the characteristics that can contribute to enhance sensor performance and expand the application of sensors in a sustainable manner. The methods to modify the surface of cellulose, including the functionalization with receptors or labelling units (such as fluorophores or redox molecules), and the fabrication methodologies for processing celluloses into functional materials are reviewed. We then introduce the progress of cellulose-based materials for the development of physical and chemical sensors and biosensors with different transduction mechanisms. We close the review by discussing the future prospects for developing cellulose-based sensors.

1.1. Cellulose Chemical Features

Cellulose, literally the sugar "ose" from cells, was firstly isolated by extraction from green plants by the French chemist Anselme Payen in 1838 [15,16]. Nonetheless, it was in the 1920s that Sponsler, Dore [17] and Haworth [18] resolved cellulose molecular structure and that Staudinger recognized its polymeric nature, giving birth to polymer science and chemistry [19].

In nature, cellulose is biosynthesized by several living organisms, spanning from higher and lower plants (i.e., algae, Valonia species), sea animals (tunicate), bacteria (Gluconacetobacter xylinus), fungi and even some amoebae (i.e., Dictyostelium discoideum) [20]. Additionally, great advances in the in vitro synthesis of cellulose [21] and the chemosynthesis of cellulose derivatives [22,23] have been achieved in the last 30 years. A single cellulose chain is a linear homopolymer composed of anhydroglucopyranose units (AGU) linked together by β-(1→4)-glycosidic linkages (Figure 1a).
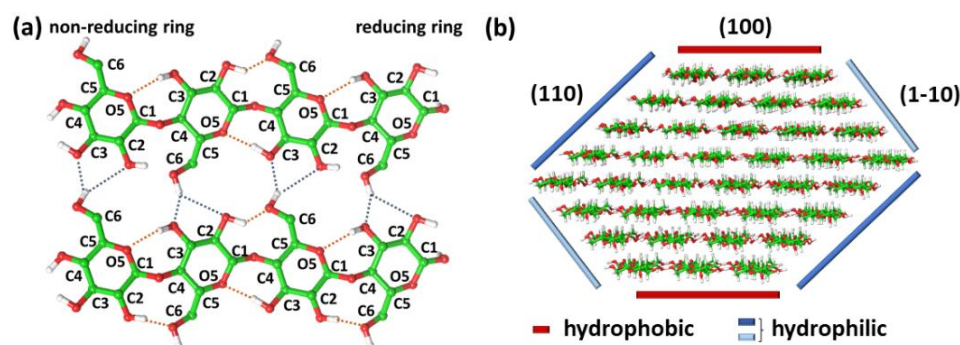

Figure 1. (**a**) Schematic representation of cellulose molecular structure and of the in-plane intrachain (orange) and interchain (dark blue) hydrogen bonds network responsible for the stable cellulose suprastructure. (**b**) Hydrophilic and hydrophobic surfaces of cellulose fibril, highlighting cellulose amphiphilic nature.

The knowledge of the molecular structure of cellulose is of prime importance to explain its characteristic physicochemical properties, such as hydrophilicity, chirality, biodegradability and high functionality. Indeed, the presence of three equatorial hydroxyl groups in each AGU—the two secondary alcohols in position C2 and C3, and the primary alcohol, the hydroxymethyl group, in position C5—donate chirality and hydrophilic properties to cellulose. Additionally, the numerous axial C-H present in the sugar rings give a hydrophobic character to the polymer [20,24]. In addition, the chemical difference of the two ends of the molecule—the non-reducing (C4-OH group) and reducing (C1-OH group) ends—provides the polarity character to the cellulose chain, which also confers interesting properties to the crystalline architecture and chain alignments (i.e., polar or antipolar) [25]. For these reasons, cellulose exhibits an amphiphilic nature and an intrinsic structural anisotropy (Figure 1a,b) [20,24].

1.2. The Hierarchical Structure of Cellulose—From Single Chains to Cellulose Fibers

The size of cellulose polymeric chains is defined by the average degree of polymerization (DP), while the product of the average DP and the molecular mass of a single AGU defines the cellulose molecular weight [26,27]. Cellulose chains present a variability of DP depending on the sources [28]. For example, native celluloses in wood pulp have a DP ranging between 300 and 1700, while cotton and bacterial cellulose have DP values in the range of 800–1000 and cellulose regenerate fibers present 250 to 500 repeating D-glucose units per chain [20]. Additionally, plant cellulose DP depends on the part of the plant from which it is extracted [29]. To date, plant-derived cellulose is produced from mechanochemical extraction from six main plant sections (i.e., bast, core, grass, reed, leaf and seed) [30] but, as a general note, cellulose DP is always reduced by purification processes [30].

In the plant cell wall, cellulose is usually combined with lignin, hemicelluloses (arabinoxylan, xyloglucan and high-molecular weight mixed-linkage glucan) [31], pectin and water (Figure 2a(i)). Conversely, cellulose extracted from other sources, such as bacteria, is highly pure with a high water content [20]. Native cellulose is organized in a hierarchal fashion (from a single AGU to cellulose fibers), where cellulose chains are held together by an extensive network of intra- and inter-chains hydrogen bonds (Figure 1a) [24]. Structurally, cellulose is a semi-crystalline polymer where the basic crystalline components are linked together by disordered amorphous domains to form cellulose microfibrils, often referred to as microfibrillated cellulose (MFC—Figure 2a(ii),b(i)) [11]. The amorphous regions give rise to some imperfections/dislocations along the microfibril length at the interface of microcrystalline domains. In turn, cellulose microfibrils aggregate to form cellulose fibers, which are aligned with the cell axis in a super-helicoidal structure to form the plant cell wall [24].

The extraction of cellulose microfibrils from bark, wood or leaves is performed by a combination of enzyme (i.e., cellulase-catalyzed hydrolysis) or chemical pre-treatment of the raw fibers [20,25]. In particular, milling and bleaching remove lignin and hemicelluloses, while processes such as contact with ionic liquids [32], TEMPO-oxidation [33] and ultrasonication [34] enhance fibrils accessibility. These pre-treatment steps can be followed by the cellulose fibrils' disintegration (mechanical shearing at high pressure) and/or hydrolysis (acid treatment) to form nanocellulose structures (Figure 2a(iii),b(ii–iv)) [30]. Importantly, if performed correctly, these steps preserve the cellulose semicrystalline structure and native crystal form [20]. Due to its fibrillated structure and the high water hold capacity, MFC is able to form hydrogels with competitive properties in comparison to other artificial polymers, such as high yield stress and viscosity, a shear-thinning behavior and a high water holding capacity [30]. The extraction and processing of MFC has been widely developed in the industry to manufacture paper and textiles [20,35].

Cellulose microfibrils present a ribbon-like shape with a flattened rectangle cross-section, which donates amphiphilic properties to MFC surface thanks to both (i) the presence of the hydroxyl groups pointing outwards the short edges of the cross-section and (ii) the C-H groups displayed at the broad edges of the cross-section and perpendicular to the main plane of the glucose ring (Figure 1b) [24]. The existence of these surfaces donates to cellulose an efficient lateral packing propensity, as bricks in a wall [25].

Depending on the sources, cellulose microfibrils present a great variation in their dimensions (length and diameter) [24]. In these fibrils, two different environments can be identified: (i) the surface chains which are accessible and reactive to molecule in solution and (ii) the chains within the crystal (bulk chains), which are instead densely packed and inaccessible without breaking cellulose organization. Indeed, surface chains have a greater conformational freedom in comparison to bulk chains, given their fewer hydrogen bond interactions. For these reasons, cellulose surface chains are partially disorganized, have higher chemical reactivity and have affinity for adsorbed species, such as water molecules, hemicelluloses and lignins [24]. Hence, when the cellulose structure is maintained, only the surface hydroxyl groups react with external reagent and cellulose derivatization occurs exclusively on the surface [24].
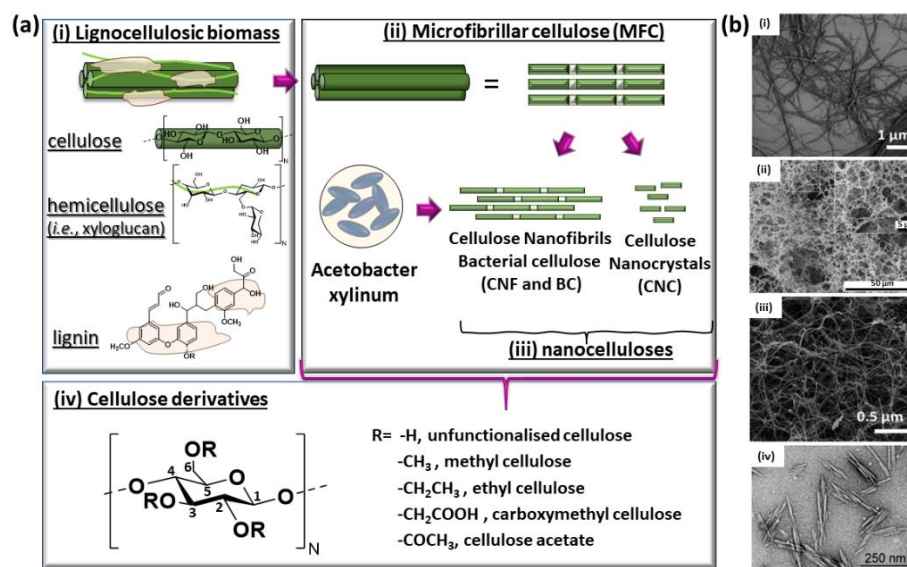
Figure 2. (**a**) Schematic representation of (i) the components of lignocellulosic biomass in plant cell wall (PCW) divided in cellulose, hemicelluloses and lignin, (ii) microfibrillated cellulose (MFC), (iii) nanocelluloses and (iv) cellulose derivatives. (**b**) Scanning electron microscopy (SEM) or transmission electron microscopy (TEM) images illustrating the morphology of different cellulose forms: (i) SEM of microfibrillated cellulose (MFC) [30], (ii) SEM of cellulose nanofibrils (CNFs) [30], (iii) SEM of bacterial cellulose (BC) [30] and (iv) TEM of cellulose nanocrystals (CNC) from cotton [36]. Copyrights: all images have been adapted and reproduced with permission from: (**b**) (i–iii) © The Royal Society of Chemistry 2020, (iv) © The Royal Society of Chemistry 2010.

2. The Great Variety of Cellulose Types and Properties

Recent studies demonstrate that celluloses present withstanding physicochemical and mechanical properties for the production of various environmentally friendly cellulose-based functional materials, including mesoporous cellulose structures, transparent thin films with high flexibility, hydrogels and aerogels. The different forms of celluloses, from either plant or bacterial sources, processed and/or functionalized, are inherently safe, non-toxic and environmentally friendly. For these reasons, cellulose and its derivatives have the potential to revolutionize the material and biomedical fields with their applications. Herein, we summarize the different kinds of today existing celluloses, making a distinction based on (i) allomorphic form, (ii) nanocelluloses and (iii) cellulose derivatives with surface or chains functionalization.

2.1. Cellulose Allomorphs

The crystal structure of cellulose has been investigated for more than a century, with Nishikawa and Ono being the firsts to obtain X-ray diffraction traces from wood, hemp and bamboo [37]. Cellulose can exist in six different allomorphic forms, namely Iα, Iβ, II, IIIi, IIIii, IVi and IVii [20]. Cellulose Iα and Iβ are the native forms of cellulose found in plants and in primitive microorganisms [37,38]. The other allomorphs, on the contrary, are obtained from diverse thermochemical treatments of cellulose Iα and Iβ. Indeed, both cellulose native allomorphs (Iα and Iβ) can be converted, in an irreversible manner, into cellulose II through mercerization or regeneration [39] or into cellulose IIIi by treatment with liquid ammonia and other amines [40,41]. Cellulose II is thermodynamically the most stable crystalline form of cellulose. Cellulose IV, also called "high-temperature cellulose", is prepared from cellulose II or III by treatment in glycerol at 260 °C. Interestingly, cellulose I cannot be transformed directly into cellulose IV [42]. The allomorph cellulose IVi is exclusively formed from cellulose IIIi treatment, while the allomorph cellulose IVii is obtained from both cellulose II and IIIii as source material. Recently, cellulose IVi has been re-classified as Iβ [42]. Nishiyama et al. revised the crystallographic structures of cellulose

and reported the H-bond networks by applying synchrotron X-ray and neutron diffraction studies [37–39,41–43].

2.2. Nanocelluloses

Nanocelluloses are commonly produced from wood pulps and residual paper fibers, bacteria or tunicates. Nanocelluloses from different sources have different characteristics, including different purity, morphology, nano-dimension geometry and crystallinity [44]. Basically, nanocelluloses are classified into two families according to their length, diameter and aspect ratio.

2.2.1. Cellulose Nanofibers (CNFs) and Bacterial Cellulose (BC) Fibers

CNFs are celluloses produced by either mechanical (i.e., high-pressure, grinding, homogenization, cryo-crushing and refining) and/or chemical (i.e., alkali treatments of fibers, the steam explosion of alkali-treated fibers, bleaching and acid treatment) methods from plant and tunicate sources [45]. Chemical treatments during CNFs extraction can lead to surface functionalization. For example, TEMPO-oxidation introduces a large amount of carboxylate groups into the cellulose nanofibers [46]. CNFs are semicrystalline and present a web-like structure with the fibers' diameter ranging from ~5 to 20 nm and a length from 0.5 to 2 μm (high aspect ratio), high flexibility and large surface area. CNFs present high strength (1 to 3 GPa) and crystal modulus (~138 GPa), low density (~1.5 g cm^{-3}) and can form viscous and shear-thinning aqueous gels with very low dry content (between 2 and 7% w/w). In addition, CNFs form transparent films upon solvent evaporation [30].

BC fibers are synthesized from several bacteria (most commonly from *Gluconaetobacter xylinus* and *Acetobacter xylinum*) with high yield, high DP (up to 8000), high purity (BCs do not require chemical processing for the elimination of lignin and hemicelluloses) and high crystallinity (84–89%). In addition, BCs present chemical purity, as they exclusively present hydroxyl groups on their surfaces. BCs are ribbon-shaped fibrils which have uniaxial orientation, high elastic modulus and elevated water holding capacity (they are able to create a 3D network and, in turn, hydrogels) and, when compressed into sheets, they present a highly planar orientation. Due to their high purity and withstanding mechanical properties, BCs are commonly used for biomedical applications, such as tissue and bone growth. Nonetheless, BC fibrils are tightly packed with a dense mesh, thus limiting opportunities for cell growth [30].

2.2.2. Cellulose Nanocrystals (CNCs)

CNCs can be isolated from many sources, including wood, hemp, algal and bacterial cellulose. CNCs are produced from MFCs and CNFs by hydrolysis of their amorphous regions with concentrated hydrochloric or sulfuric acids. The amorphous regions present a higher susceptibility to breakdown at the glycosidic bonds level, which results in a longitudinal cleavage of the cellulose microfibrils and nanofibers, yielding shorted crystalline moieties. CNC nanoparticles are therefore highly crystalline and present a needle-like morphology with a diameter of 3–7 nm and a length of ~100 nm [30].

The introduction of negative charges on the CNCs' surface could occur under certain hydrolysis conditions, which in turn highly influence the CNCs' properties. Hydrolysis with hydrochloric acid results in the degradation of the amorphous phase but does not introduce negative charges, so that CNCs are not stable in a water dispersion and the suspension flocculate [47]. On the contrary, hydrolysis with sulfuric acid results in charged sulphate groups on the CNCs' surface, and the resulting dispersions are very stable in water. Nonetheless, these sulphate groups are labile and rapidly removed under mild alkaline conditions [44]. An alternative route for the introduction of more stable negative charges on the CNCs' surface is TEMPO-mediated oxidation, which involves the selective conversion of the surface hydroxymethyl groups into carboxylic groups while maintaining the cellulose morphological integrity and native crystallinity [33,46].

CNCs present an elastic modulus comparable with CNFs (up to 140 GPa), but their shorter length and higher crystallinity are a drawback in terms of flexibility [48]. In water, the CNCs' suspension can form, beyond a critical concentration, an anisotropic chiral nematic liquid crystal phase. The CNCs' large surface area and rod-like shape make them a good material for film/membrane preparation [25]. Favored by the nanoscale dimension, high crystallinity and competitive elastic modulus, CNCs mostly find application as reinforcement polymer in nanocomposites [49]. In addition, the appropriate modification of the CNCs' surface can donate outstanding and tailored physical, chemical, biological and electronic properties to this material, enlarging the span of its applications [30].

2.2.3. Cellulose Derivatives

It was the Hyatt Manufacturing Company, in 1870, which paved the way to industrial scale production of chemically functionalized cellulose by-synthesizing cellulose nitrate via reaction with nitric acid [20]. From that point onwards, the engineering of cellulose surface and, in turn, its interfacial properties have become of paramount importance in the development of assembled materials for various applications. For these reasons, a large variety of strategies have been developed and applied to functionalize cellulose surface. In general, either heterogeneous or homogeneous functionalization of cellulose can be achieved, depending on the working conditions. In the first case, cellulose is in a swollen state and the microfibrillar nature of cellulose hinders the access to some hydroxyl groups. Depending on the type of solvent used, the cellulose's fibrous morphology can be retained or considerably changed, according to the occurrence of disruption of interchain hydrogen bonds during swelling [24]. In the second scenario, the homogeneous functionalization strategy, cellulose is completely dissolved in solution, and the functionalization is achieved through all the cellulose single chains [20].

Given the inherent cellulose insolubility in water and in most organic solvents (i.e., trifluoroacetic acid, dimethyl sulfoxide or *N,N*-dimethylacetamide) [24], heterogeneous methods are the ones applied for the production of most commercially available cellulose derivatives. Nonetheless, homogeneous methods are important to finely control the total degree of substitution and to introduce new functional groups, opening new avenues in product design. For these reasons, the strategies for the complete dissolution of cellulose have been on the focus [50], although mostly relying on the use of unusual solvents with high ionic strength and harsh conditions. Nonetheless, ionic liquids have recently appeared as a "green" alternative for cellulose dissolution [32].

Industrially important chemical modifications of cellulose generally involve a reaction with its 2-, 3- and 6-hydroxyl groups (Figure 2a(iv)) [25]. These hydroxyl groups present different reactivity depending on their degree of organization and the establishment of hydrogen bonds. Specifically, hydroxyl groups in an amorphous structure have similar accessibility and therefore the same reactivity, while those in a crystalline structure will present a reactivity influenced by their degree of organization. Indeed, a study conducted by Rowland et al. [51] on cellulose samples with different degrees of crystallinities demonstrated a correlation between the crystallite index of the cellulose samples and the hydroxyl groups accessibility. In particular, 2-hydroxyl groups are generally the most accessible. In contrast, the 3-OH group is the least accessible to chemical agents in highly crystalline Valonia or bacterial celluloses, while it presents a higher reactivity in cotton cellulose where the degree of organization is less perfect. The 6-hydroxyl group shows an intermediate reactivity, also depending on the crystallinity index of the cellulose.

The reactivity of the hydroxyl group is highly correlated with the hydrogen-bonding network of cellulose. Indeed, the lack of reactivity of the 3-hydroxyl group suggests that the strong 3-OH$\cdots$O-5 hydrogen bond observed in the crystalline structure persists at the cellulose surface of the cellulose materials, whereas the higher reactivity of the 2-OH and 6-OH groups suggests that the hydrogen bonds involving these groups are partially disrupted at the surface (ref. to Figure 1a for the H-bond network). In addition, the difference in reactivity between the hydroxymethyl group and 2-OH can be explained

by their chemical diversity. Indeed, the hydroxyl group in C6 is highly accessible, while the hydroxyl in C2 is highly acidic and in close proximity to the acetal function [25]. The described reaction sites undergo most of the common reactions of alcohols, such as oxidation, etherification, acylation (formation of esters) and deoxygenation. Among these, etherification and esterification are particularly important and have been frequently used for cellulose functionalization [25].

The etherification of cellulose can be achieved using alkyl halides in the presence of a strong base (Williamson ether synthesis), this strategy being commonly used to produce carboxymethyl, hydroxypropyl and hydroxyethyl celluloses [24]. Alternatively, ether formation from unsaturated compounds can be achieved by Michael addition [25]. Cellulose esters, such as cellulose formate, cellulose acetate or cellulose nitrate, are usually synthetized by acylation with the appropriate acid, its anhydride or its acid chloride in the presence of an activating agent (i.e., *N,N*-dicyclohexylcarbodiimide, DCC) and a basic catalyst (i.e., pyridine or thiethylamine) [25].

The deoxygenation reaction of cellulose involves the removal of the 2-, 3- or 6-OH group and its replacement with a different group with no oxygen directly attached to that cellulose position. For example, the replacement of the 6-OH with an aliphatic diamine produced the so-called aminocellulose derivatives, which will be further discussed due to their application in bio coupling [3].

Finally, oxidation reactions can be accomplished either at the hydroxymethyl group level (6-OH) or at the C-2 and C-3 levels. Oxidation of the hydroxyl group in C6 involves the use of nitroxy radicals, such as the well-known 2,2,6,6-tetramethylpiperidine-1-oxy radical (TEMPO), which oxidizes the primary hydroxyl group to a carboxyl group in a regioselective manner [52,53]. The introduction of this new functional group allows for the further derivatization via amide coupling by using *N*-ethyl-*N*-3-(3-dimethylaminopropyl) carbodiimide (EDC) and *N*-hydroxysuccinimide (NHS). This strategy has been used to couple the carboxyl groups of oxidized cellulose with an amine derivative, such as aminated polymers [54], amino acids [55], peptides [56] and proteins [57].

In contrast, the oxidative cleavage of the C-2 and C-3 bonds leads to the formation of the corresponding dialdehyde, which can be further oxidized to a diacid or reduced to a dialcohol. The oxidation can be performed either by sodium periodate ($NaIO_4$) [58] or by ceric ammonium nitrate (CAN) [59]. In the first case, the oxidized cellulose can be further derived by amination reaction into an imino-cellulose, which can be further reduced using agents such as $NaBH_3CN$ [60]. The second oxidation process, instead, leads to the formation of an aldehyde group and a radical function on a carbon atom bearing a hydroxyl group. The resulting compounds can be further polymerized with acrylonitrile to form cellulose–polyacrylonitrile graft copolymer [59].

Besides chemical functionalization of bulk cellulose, many attempts and advances have been made in its in vitro ex-novo synthesis, which could guarantee a more defined regiocontrol in cellulose functionalization and, in turn, self-assembly. Bottom-up processes include the production of bacterial nanocellulose from glucose by bacteria, as well as chemoenzymatic approaches and solid-state synthesis. In the context of chemoenzymatic approaches, the loose specificity of some enzymes allows for the introduction of modifications along the cellulose chain [23]. For example, cellodextrin phosphorylase from *Ruminoclostridium thermocellum* has been used for the synthesis of glucosamine derivatives of cellulose type II [61], as well as for the decoration of cellodextrin chains with fluorine atoms in a regiocontrolled manner, giving rise to a new cellulose allomorph [22]. Finally, advances in the solid-state synthesis of cellulose and its derivatives, such as the glycosynthesizer developed by Seeberger et al., allows for the fine decoration of cellodextrin chain with high regioselective control [62].

3. Cellulose-Based Materials

The great variety of existing cellulose forms, the high molecular weight of the polymer and its ability to form 3D networks give rise to various morphologies and assembled

materials in the form of sheets, fibers and globular particles (Figure 3). These structures are generally held together by a fine balance of supramolecular forces, such as hydrogen bonding and hydrophobic interactions. In addition, different processes, for example freeze-drying, solution casting and evaporating as well as 3D printing and spinning, lead to the production of various cellulose formulations (i.e., cellulose aerogels, films/membranes and fibers, respectively). Each one of these formulations presents characteristic properties, which are important for the development of different sensing strategies. Herein, we report an overview of the most common forms in which cellulose is formulated.
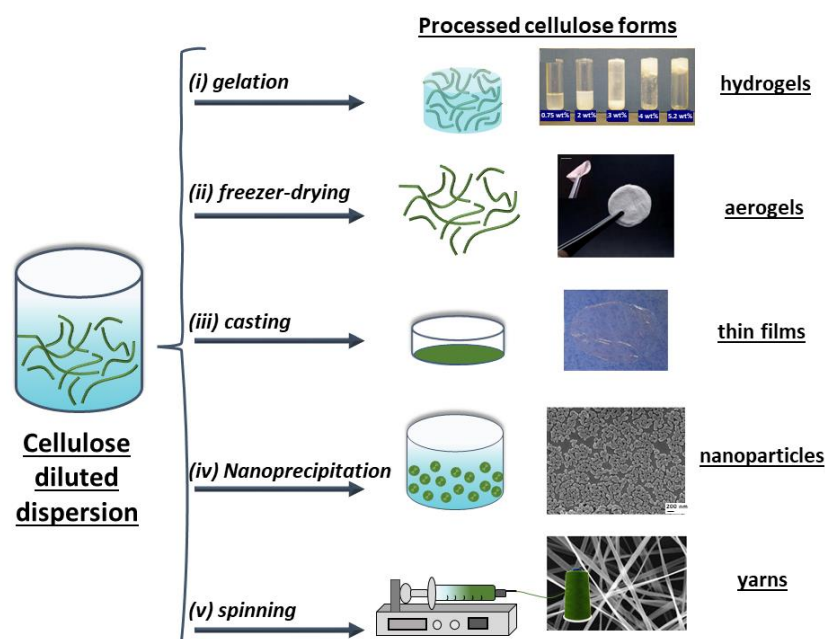

Figure 3. Representation of different approaches for processing cellulose dispersions resulting in (i) hydrogels from cotton CNC suspensions at different CNC concentrations [63], (ii) highly flexible CNF aerogel formed by freezer-drying of a CNF hydrogel [64], (iii) thin films prepared from a 10-times homogenized dispersion of MFC 0.13 wt% [65], (iv) nanoparticles of cellulose acetate (CA) formed by the dropwise adding of water into an 4 mg CA/mL acetone solution [66] and (v) SEM images of cellulose acetate (CA) yarns prepared by electrospinning 17 wt% CA solution in acetone/water (85/15 *v*/*v*) solution [67]. Copyrights: all images have been adapted and reproduced with permission from: (i) © 2014 Wiley Periodicals, Inc (ii) © The Royal Society of Chemistry 2011, (iii) © Springer Science+Business Media B.V. 2010, (iv) © 2008, American Chemical Society, (v) © 2004, American Chemical Society.

3.1. Cellulose Hydrogels (CHGs)

Hydrogels are soft matter systems which present a solid-like behavior even though they are mostly composed by water. The ability of hydrogels to preserve a solid form has been attributed to the creation of cross-links between the gelator molecules, which results into a gelator 3D network, as well as to the propensity of water to interact with the formed network [68]. The ability of cellulose to form a 3D network thanks to its fibrillar form and/or to the establishment of several supramolecular interactions, such as hydrogen bonds and van der Waals interactions, has been widely exploited for the formulation of hydrogels. Indeed, cellulose-based hydrogels have been on the sight for more than three decades, and roughly all the celluloses in their possible forms (MFC, nanocelluloses, cellulose derivatives) are able to hold high amounts of water and preserve a solid-like behavior (Figure 3(i)).

Cellulose is able to produce hydrogels alone, by modulation of its concentration [63,69] and/or the solution pH [70], in composite systems [71] or in the presence of additives, such as salt [72], surfactant [73] or alcohols [74]. For example, the introduction of carboxyl

functional groups into the cellulose chain/surface, as in the case of carboxymethyl cellulose or TEMPO-oxidized nanocelluloses, allows for the formulation of reversible hydrogels based on the formation of metal ion coordination complexes [72,75]. Indeed, the addition of salts reduces the Debye length of anionic cellulose derivatives and, in turn, suppresses electrostatic repulsion between the cellulose chains. The cellulose propensity to form gels can also be enhanced by the use of cosolvents, i.e., alcohols, in addition to water. For example, the ability of TEMPO-oxidized CNFs to gelate in the presence of methanol, ethanol and propanol has been reported and the mechanism of gelation thoroughly studied both from the perspective of fibrils overlapping [74] and water structuration [68].

Cellulose-based hydrogels possess attractive properties for the development of sensors. Indeed, on top of their inherent biocompatibility, biodegradability and renewability, they present excellent mechanical performances, such as high strength and high toughness [76].

3.2. Cellulose Aerogels (CAGs)

Aerogels are lightweight, porous, solvent-free materials typically prepared from solvent swollen gels or polymeric solutions [77]. Importantly, for aerogel formulation, the uncontrolled collapse of the network during solvent removal must be avoided. To this end, freeze-drying, solvent exchange with ethanol and supercritical CO_2 drying have usually been performed in cellulose dispersions and hydrogels to obtain the respective aerogel [77]. Cellulose aerogels (Figure 3(ii)) are typically formed by MFCs [78], CNFs [79,80] or BCs [81,82] due to their fibrillar form, although formulations of aerogels from CNCs have also been reported [36]. In particular, the resulting porosity, density, surface area and morphology (from nanofibrillar to sheet-like skeletons) depend on the starting material and on the process used for solvent removal [79]. Cellulose aerogels find application in various fields, including thermal and acoustic isolation, templating and catalyst supports [36]. For example, electroconductive CNF-based aerogels were obtained from the incorporation of an electrically conducting polyaniline-surfactant solution into the CNF matrix and subsequent removal of unbound molecules [79]. In addition, due to their competitive properties, cellulose aerogels are good candidates for the further development of aerogel-based sensors [83].

3.3. Cellulose Films (CFs)

Cellulose has been demonstrated to be a great film-forming material. The most common and famous film constituted of cellulose is paper, classified as a random fiber network [84] or as an orthotropic continuous medium [85] held together by hydrogen bonds [86,87]. Paper sheets are not exclusively constituted by cellulose microfibril, but also by pectin and hemicelluloses. The presence of these additional components, which act as binders between the MFCs, highly influence the paper/sheet mechanical behavior, such as the load transfer when subjected to stress. For these reasons, pulp extraction processes have to be carefully considered. For example, in a work reported by Dufresne et al., it was demonstrated that pectin removal decreased the tensile modulus of films made from sugar beet pulp in dry atmosphere [88]. Importantly, paper finds extensive use in the formulation of disposable sensors for on-site testing in POC devices (for further details, we refer the reader to the reviews published by the research groups of Güder [48] and Golmohammadi [89]), and as a substrate for electrochemical micro devices [35].

Generally, cellulose film formulation is subsequent to the cellulose purification and derivatization steps. In particular, cellulose derivatization is often carried out to improve its solubility [90]. For example, the production of another very famous transparent cellulose film, cellophane, involves cellulose derivatization into sodium cellulose xanthate, which is then reconverted into cellulose II or regenerated cellulose [91]. Additional common film-forming cellulose derivatives are cellulose acetate, methyl cellulose and carboxymethyl cellulose [91].

More recently, nano-paper attracted attention in various fields, including (bio)sensing technology [89]. Hence, particular attention must be given to nanocelluloses (BC, CNFs and

CNCs), which can be formulated into thin films (Figure 3(iii)). Importantly, differences in self-assembly lead to films with different optical properties, spreading from transparency to scattering and to photonic pigments [44,92]. Nanocellulose films are generally produced by evaporation-induced self-assemblies upon solvent-phase removal (film casting). Additional routes for film formulation involve spin coating and the Langmuir–Blodgett techniques [90].

Thin films made of pure CNFs are optically transparent [93], have low density and high tensile strength (σ = 250–350 MPa) with strain to failure reaching ε = 10% [94]. On the other hand, pure films of CNCs present special optic features given the propensity of these colloidal particles to organize into a liquid crystalline (LC) phase. Indeed, it is well known that, above a certain concentration, CNCs spontaneously organize into a cholesteric LC phase with chiral nematic order, which is preserved upon drying. Hence, this supramolecular assembly gives rise to helicoidal structures in the solid state, resulting in an iridescent structural color which depends on the pitch (p), the average refractive index (n) and the orientation of the helical axis (m) [95,96]. Nonetheless, given the formation of grain boundaries which promote crack propagation, these films are generally brittle [97]. Recently, the formulation of self-standing thin film with competitive mechanical properties with TEMPO-oxidized CNCs was reported [55]. In addition, to push the boundaries of the CNC films' mechanical performance, additional supramolecular binding motifs can be introduced on the CNCs' surface upon functionalization. For example, the introduction of simple amino acids into the TEMPO-oxidized CNCs' surface leads to films with competitive mechanical properties, tailored by the delicate balance within the already present supracolloidal nanocellulose–nanocellulose interactions and the newly introduced supramolecular forces (i.e., electrostatic repulsion, π–π-stacking and cation-π interactions) [55].

3.4. Cellulose Nanoparticles (CNPs)

Since the first report by Ragauskas et al. in 2007 [98], the CNPs field has expanded from non-functionalized cellulose [99] to nano amino cellulose [100], nano carboxycellulose [101,102], cellulose acetate [66,103] and composites [104]. Cellulose nanoparticles (Figure 3(iv)) can be formulated by homogenous processes involving the dissolution of the cellulose I amorphous regions with acid hydrolysis [105], or by acid-free heterogeneous processes, with the consequent preservation of the original crystalline structure and of the amorphous regions [106] followed by nanoprecipitation [107]. CNPs are highly hydrophilic spherical particles with diameters ranging from 100 to 500 nm [98], which can present either amorphous and/or crystalline structures and show specific chemicophysical properties, such as good accessibility, high functional group content and sorption ability [102]. CNPs are typically used for the immobilization of active pharmaceutical ingredients or as fillers in pharmaceutical formulations and cosmetics, as well as supporting materials for catalysis and enzymes for biosensing [102,108].

3.5. Spun Celluloses or Cellulose Yarns (CYs)

The formulation of celluloses via processes such as wet spinning [109], dry spinning [109], melt spinning [110] or electrospinning [111] results in the construction of fibril-like, filamentous structures (Figure 3(v)). In order to obtain fibers with reproducible sizes and properties, a careful selection of solvents and co-solvents as well as an optimization of the formulating parameters (i.e., solution viscosity and shear rate) are required. Usually, soluble cellulose derivatives (for example, cellulose acetate and hydroxypropyl cellulose) are used in spinning techniques. The formulation of celluloses via spinning techniques makes it possible to modulate the fibers and the filaments' degree of alignment, which in turn translates into tailored mechanical properties, such as changes in the fibrils Young's modulus and stress at break [112]. Indeed, in nature, plant cell wall strength highly correlates with the angle between cellulose microfibrils axis: where higher stiffness is required, fibrils show a lower angle, and vice versa. An explanation can be found in the anisotropy of cellulose crystallites, which present a Young's modulus up to 160 GPa and 8–57 GPa in the longitudinal and in the transverse directions, respectively [113].

4. Cellulose in (Bio)Sensing

The aforementioned features of the various cellulose formulations reflect into cellulose applicability as a platform for (bio)sensing. In fact, celluloses are excellent scaffolds for hosting various nanomaterials, such as plasmonic NPs, photoluminescent NPs, carbon nanotubes, as well as biological receptors such as proteins, from antibodies to enzymes and DNA/aptamers. Furthermore, cellulose nanocrystals can act as signal transducer themselves due to the optic properties of the cholesteric phase. For these reasons, cellulose-based hybrid materials have been employed for the fabrication of sensors for various applications, ranging from biochemical sensing (from gases and ions to drugs, biomarkers and pathogens) to physical sensing (i.e., strain, proximity and pressure sensors) and humidity sensing.

Herein, details of cellulose application in (bio)sensing will be discussed, with a focus on which form of cellulose is most appropriate for each sensing strategy. We will try to answer the following questions: (1) why does the use of cellulose lead into advances in the sensor fabrication and (2) which kind of cellulose should be used to develop a sensor with defined functions. To do so, for each of the reported sensing strategies we will show a few selected examples of cellulose applied in sensor development.

To help the reader, we divided this section of the review into the most common employed (bio)sensing strategies (i.e., optical and electrochemical sensing). Given the extensive use of cellulose, a comprehensive description of all the cellulose-based systems developed for each sensing strategy is beyond the scope of this review. For further details, we will address the reader to specific reviews of different sensing approaches.

4.1. Cellulose in Optical (Bio)Sensing

In this section, some examples of cellulose used in optical sensing, including surface-enhanced Raman scattering (SERS), fluorescent and colorimetric methods, nanoplasmonic systems and surface plasmon resonance (SPR) will be discussed.

4.1.1. Surface-Enhanced Raman Scattering (SERS)

Given its high selectivity and sensitivity, SERS is nowadays considered one of the most powerful tools for (bio)chemical detection. Thanks to its unique properties, cellulose is an important component in the design of SERS substrates. In particular, cellulose can act as a reducing component for the preparation of plasmonic nanoparticles and as host of NPs for SERS applications. Indeed, nanostructured metals, such as Au, Ag and Cu, have been reported to generate a strong surface plasmon resonance (SPR) in the visible and near-infrared regions. These NPs give rise to local surface plasmon resonance (LSPR) which, in turn, generate SERS hotspots—highly localized regions of intense local field where the signal of adsorbed molecules is enhanced with factors higher than 10^6. Importantly, signal enhancement is highly affected by composition, shape, size and interparticle spacing of the noble metal NPs [114,115]. For these reasons, metal NPs embedding into a porous and flexible substrate has been researched as a strategy to maximize the SERS number of hotspots.

Metal nanoparticles are generally synthesized by the reduction in the corresponding metal salt with reducing agents such as $NaBH_4$, hydrazine (NH_2NH_2), hydroxyl amine (NH_2OH), triethanol amine (TEA), poly(ethylene imine) (PEI), and dimethylformamide (DMF) [115]. The nanoparticles are then stabilized in a polymeric matrix, commonly composed by polyvinylpyrrolidone (PVP), poly(ethylene glycol)-block-poly(propylene glycol)-block-poly(ethylene glycol) or silanes. The introduction of functional groups into the polymeric scaffold (i.e., thiol, carboxylic acid and/or amino groups) can anchor the metal nanoparticles and minimize aggregation. Tannic acid and sodium citrate have been widely used both as reducing and stabilizing agents in the synthesis of metal nanoparticles [116]. Nonetheless, the use of reducing chemical agents can generate by-products, while some polymers used as SERS matrix give interference and background signals during signal acquisition [115].

In these regards, cellulose has been demonstrated to be an optimal platform due to its minimal SERS signal interference, high stabilization performance and, when functionalized, its ability to control the growth of metal nanoparticles with various shapes and dimensions. In particular, fibrillated celluloses (paper, MFC, CNF and BC) are able to create a flexible 3D network with tailored porosity and morphology and are, therefore, excellent platforms to prevent the agglomeration/aggregation of metal NPs.

For example, the deposition of Ag nanoparticles on paper [117,118] or cellophane [119] has been investigated to produce handy SERS substrates which have been used for the detection of organic compounds such as carbazole, 1-aminopyrene, benzoic acid, crystal violet and acetamiprid, but those systems showed low Raman signal enhancement in comparison with Ag colloids [115]. In a recent study, a significant improvement in the paper matrix mechanical and thermal stability was achieved by layering a silver–chitosan nanocomposite in paper cellulose. The formulation of this composite maximized the porosity of the paper, which translated into an increased number of hotspots and into a capability to filtrate small molecules. The fabricated system was used for the SERS detection of 4-aminothiophenol with a detection limit of 5.13 ppb [120].

Cellulose derivatives, including cellulose acetate (CA), methylcellulose (MC), nitro-cellulose, hydroxyethylcellulose (HEC) and hydroxymethylcellulose (HMC), have been employed for the preparation of SERS substrates, principally due to their ability to dissolve in organic solvents (i.e., CA dissolves in formamide–acetone solvent mixture) or water and hereafter to produce hydrogel or membranes [115]. Lately, more focus has been given to nanocelluloses and their use in sensing. The use of bacterial cellulose (BC) as a SERS substrate was firstly reported for the development of a sensor for the determination of thiosalicylic acid and 2,2-dithiodipyridine, demonstrating the BC nanofibrillar structure to be an efficient matrix for the NPs' nucleation and growth [114,121]. In addition, in a work reported by Park et al., it was shown that spatial deformation/contraction of the BC 3D network due to drying resulted in a considerable enhancement of the SERS signal intensity due to a decrease in the distance between the NPs [122]. The sensor robustness was tested for the label-free detection of 4-fluorobenzenethiol and phenylacetic acid (PAA), the last being detected even without showing any affinity for the AuNP surface thanks to the contraction of the AuNP-BC hydrogels [122].

Importantly, in addition to its ability to act as supporting matrix, it was demonstrated that celluloses are able to act as a reducing, capping and shape-regulating agent in nanoparticles synthesis. For example, it was reported that CNC is able to act as a reducing agent in a hydrothermal synthesis reaction for the formation of palladium nanoparticles [123,124]. Moreover, it was shown that negatively charged celluloses, sulfuric acid hydrolyzed CNC [125] and TEMPO-oxidized nanofibrillated celluloses [126] are able to act as capping agents in the synthesis of spherical Ag nanoparticles. Recently, cellulose nanofibers were decorated with AgNPs to yield water-dispersible plasmonic cellulose nanofibers, AgCNFs (Figure 4a(i)). The proposed synthetic approach yielded to the formation of fiber bundles that bring the AgNPs into close proximity, resulting in SERS hotspots. The rapid SERS analysis of pesticides and fungicides by this water-dispersible substrate was demonstrated (Figure 4a(ii)) [127]. In addition, Jiang et al. reported on the dual capping and shape-regulating ability of TEMPO-oxidized CNF towards AgNPs, which resulted in an effective detection of rhodamine 6G [128]. Plasmonic flower-like silver nanostructures were also prepared in aqueous solution by using 2,2,6,6-tetramethylpiperidine-1-oxyl-oxidized nanocellulose fibers (T-NCFs, or TEMPO-oxidized CNFs) and trisodium citrate (TSC) [129]. The authors demonstrated that the shape and size of flower-like Ag morphology was controlled by T-NCF, which acted as a reducing and as a capping agent, allowing for the directional growth of Ag T-NCF structures (Figure 4b).

Flexible and high sensitivity nanocellulose SERS substrates were recently fabricated and applied for the detection of pesticides directly on apple peel [130]. The SERS substrate was prepared by assembling gold nanoflowers (AuNFs) and silver-coated gold nanocubes (Au@AgNCs) on a CNC film via electrostatic adsorption (Figure 5). The obtained composite

films can be easily bent (Figure 5(ii)) thanks to the good mechanical strength and flexibility of nanocellulose films. The flexible SERS substrate allows for the detection of pesticide residues directly on the apple's surface (Figure 5(iii)), with LODs for dimethoate and acetamiprid of 4.1 and 10.7 µg/L, respectively.
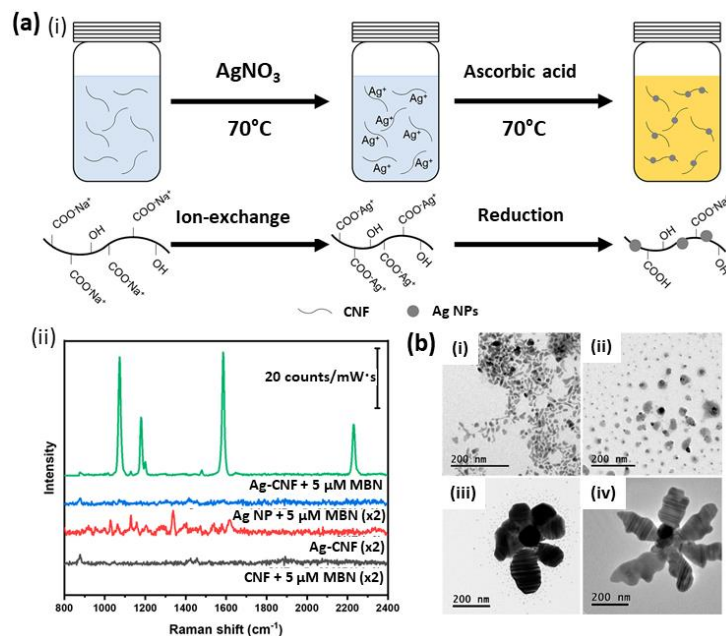

Figure 4. (**a**) Schematic representation of the in-situ synthesis of cellulose nanofibers (CNFs) decorated with AgNPs (i) to yield plasmonic cellulose nanofibers (Ag-CNFs), which serve as SERS substrate for the rapid and enhanced detection of (ii) mercaptobenzonitrile (MBN) [127]. (**b**) TEM images showing the evolution of flower-like morphology of Ag nanostructures (Ag NFs) prepared using T-NCFs, TSC and AgNO$_3$: (i) initial worm-like Ag nanostructures on T-NCF; (ii) growth of Ag nanostructures by the addition of TSC; (iii) Ag NF nanostructures after 45 min; (iv) a fully evolved flower-like morphology after 60 min [129]. Copyrights: All images have been adapted and reproduced with permission from: (**a**) © 2020, American Chemical Society; (**b**) © 2016, American Chemical Society.
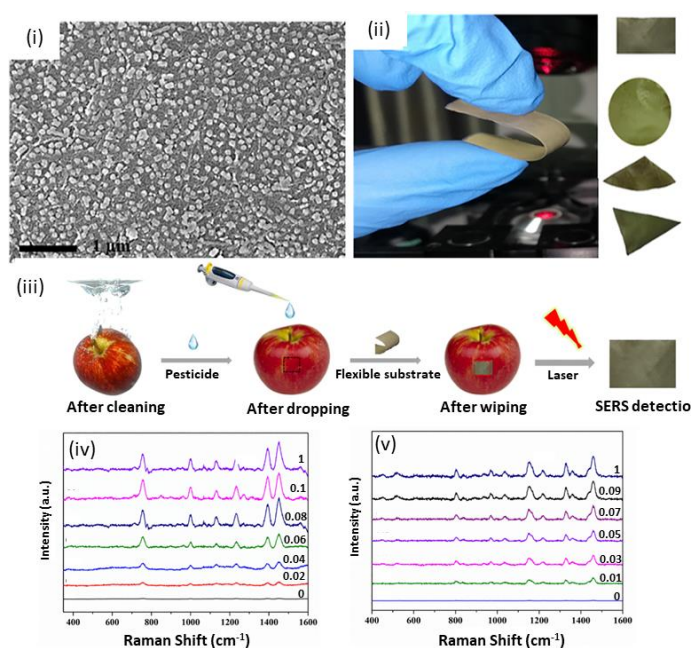

Figure 5. SEM images of CNC-S70/Au–Ag NCs prepared via self-assembly of gold nanoflowers (AuNFs) and silver-coated gold nanocubes (Au@AgNCs) on nanocrystalline cellulose (CNC) films (i) to

yield high flexible SERS substrates (ii) for the detection of pesticides on the surface of apples (iii); SERS spectra of omethoate (iv) and acetamiprid (v) on apple peel with different concentrations [130]. Copyrights: All images have been adapted and reproduced with permission from: © 2021 Elsevier Ltd.

4.1.2. Fluorimetry

The immobilization of fluorophores in a polymeric matrix has been widely used to donate analyte-dependent optical properties (i.e., fluorescence) to the polymer itself and develop highly sensitive fluorescence sensors. In this context, cellulose is an excellent matrix for fluorescence-based sensing due to its high hydroxyl content, which makes it possible to introduce fluorescent groups with high yields. Nonetheless, a pre-activation step, with oxidants such as sodium hypochlorite and sodium periodate, for example, is usually required to enhance the reactivity of the surface hydroxyl group of cellulose and therefore improve chromophore coupling [131,132].

Various fluorescent dyes [131] and photoluminescent polymers [133] coupled with cellulose have been investigated. For example, cellulose nanocrystals coupled with fluorescein-5'-isothiocyanate (FITC) and rhodamine B isothiocyanate (RBITC) resulted in a pH sensor able to detect pH ranging from pH 3.5 to pH 8.0 by measuring the fluorescence emission intensities at λ_{em} = 520 nm and 570 nm for FITC and RBITC, respectively [134]. The coupling of fibrillated bacterial cellulose with 5-(4,6-dichlorotriazinyl) aminofluorescein allowed for the sensitive detection of cellulase enzymes [135], while the coupling of electrospun cellulose acetate nanofibrous membranes with hydrolyzed poly[2-(3-thienyl) ethanol butoxy carbonyl methyl urethane] resulted in the detection of methyl viologen (MV^{2+}) and cyt c in an aqueous solution [136].

The sensitivity of fluorescence sensors is highly dependent on the interaction between the analyte and the fluorescent molecule. In comparison with other polymers, cellulose presents high processability and a large surface area, with a consequent improvement of the interaction between analytes and fluorophores. For example, the work reported by Davis et al. [137]. clearly shows how cellulose features, its fibrillar structure and ability to form a 3D network, as well as its functionalization/defunctionalization capability and its processability, can be strategically used to improve sensor performances. Indeed, the authors described the formulation of the fluorescence sensing material by the electrospinning of cellulose acetate (AC) nanofibers with an incapsulated ionic fluorescent dendrimer (Figure 6a). The AC deacetylation step enhanced the system porosity and, in turn, favored molecular interactions between the analyte and the fluorophore, which enhanced the sensitivity of the sensor. The developed system was tested for the detection of metalloproteins, including cytochrome c (cyt c), hemoglobin (Hgb) and bovine serum albumin (BSA). The first two proteins were detected by a quenching mechanism attributed to both energy and electron transfer upon interaction between the anionic dendrimers and the positive patches of such globular proteins (Figure 6b). In the case of BSA, however, an increase in fluorescence was observed, attributed to a reduction in the π-π stacking between the negatively charged dendritic fluorophores due to repulsion forces operated by the negatively charged BSA proteins (Figure 6c) [137].

Importantly, the work reported by Fontenot et al. clearly outlines the structure–function relationships of cellulose and nanocellulose-based sensors, including specific surface area (SSA), degree of substitution and transducer surface properties [138]. In particular, they described the bioactivity and related transducer surface properties of cellulose and nanocellulose matrices such as peptide–cellulose fluorescent sensors for the detection of human neutrophil elastase (HNE), a biomarker for the stalled inflammatory state of chronic wounds. The tested cellulose (filter paper and print cloth) and nanocellulose (wood cellulose nanocrystals) transducers and their composites (blends of CNC and MFC with a ratio of 66/33 and 50/50) showed a clear correlation between sensor sensitivity and film-specific surface area [138].
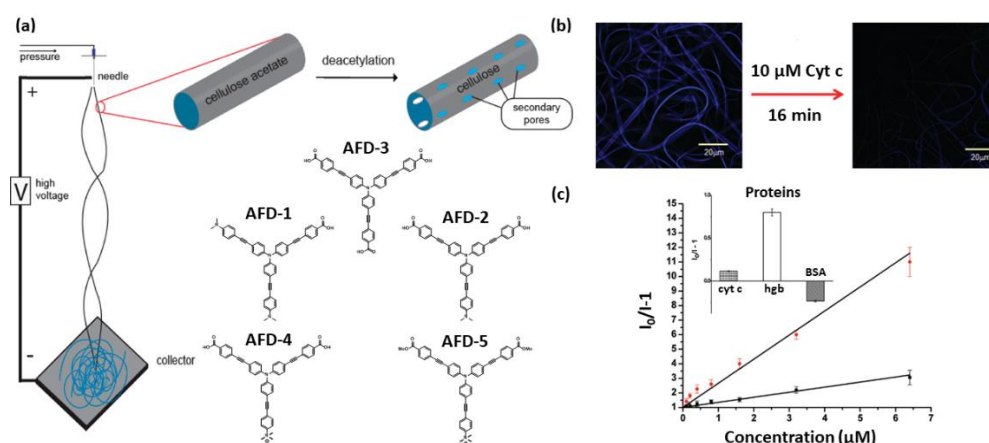
Figure 6. (**a**) Schematic representation of the preparation of electrospun nanofibers from cellulose acetate encapsulating anionic fluorescent dendrimer (AFD). (**b**) The fluorescence of the AFD-functionalized nanofibers is quenched by introduction of metalloproteins, such as cytochrome c, cyt c. (**c**) Stern–Volmer plots for cyt c (black) and Hgb (red) [137]. Copyright: images adapted and reproduced with permission from © 2010, American Chemical Society.

Electrospinning was also employed for the preparation of a microporous nanofiber film from 1,4-dihydroxyanthraquinone (1,4-DHAQ) and cellulose acetate [139]. The fluorescence intensity of the resulting film decreased linearly with the concentration of Cu^{2+} with high selectivity, indicating the potential applications of this fluorescent sensor in environmental monitoring. Paper-based fluorescent test strips for the detection of toxic nitroaromatic compound pollutants, such as 2,4,6-trinitrotoluene (TNT), were prepared by absorbing hydrophilic pyrene-functionalized polymer into cellulose-based filter papers (Figure 7a,b). Upon exposure of the contaminated sample to the test strips, the paper substrate allows for an ultrafast and spontaneous capillary force driving diffusion of TNT into the hydrophilic matrix, resulting in an efficient quenching of pyrene. This paper-based test strip enables both the fluorescent and naked-eye (Figure 7c) detection of TNT even at a low-ppm level [140].
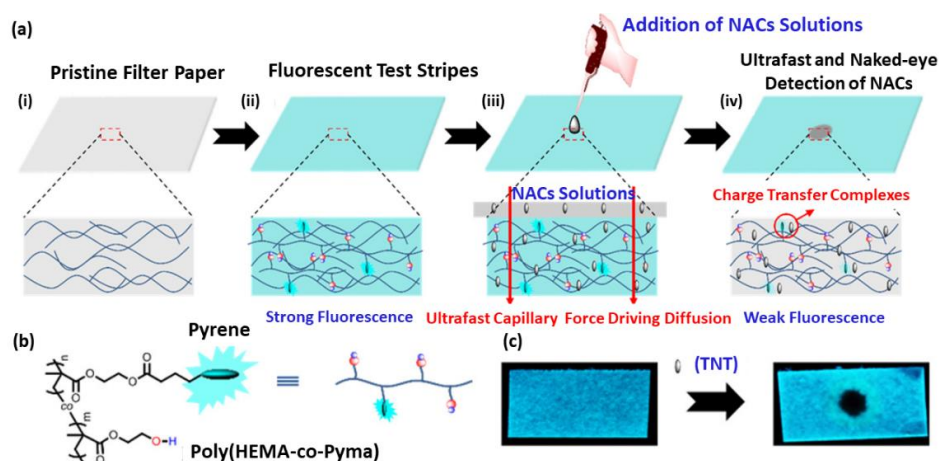

Figure 7. (**a**) Schematic representation of the preparation of a paper-based fluorescent test strip by absorbing hydrophilic pyrene-functionalized polymer into cellulose-based filter papers (i), followed by drying it (ii). The resulting fluorescent paper sensor was used for the detection of nitroaromatic compound (NAC) pollutants, consisting in the NAC-induced quenching of pyrene excimer emission (iii,iv). (**b**) Structures of the pyrene-functionalized polymer poly (HEMA-co-PyMA). (**c**) Fluorescence response (under UV lamp at 365 nm) of the paper-based sensor for detection of 25 ppm TNT sample in aqueous solution [140]. Copyright: images adapted and reproduced with permission from © 2017, American Chemical Society.

It should be highlighted that, besides its capability to form functionalized films suitable as transducer surface, cellulose can also play an active role in the recognition process. For example, the natural chirality of cellulose has been exploited in the design of a chiral fluorescence sensor for aromatic nitro compounds containing central and axial chirality [141]. Indeed, it is well known that benzoate and phenylcarbamate derivatives of cellulose show excellent chiral discrimination for racemates, such as amino acids, π-basic or π-acidic aromatic compounds, with different types of chirality (central, axial, planar, helical and topological chirality) [142]. Hence, a cellulose derivative bearing π-conjugated terthienyl pendants as fluorescent signaling units has been developed, resulting in a chiral fluorescent sensor capable of discriminating various types of chirality in aromatic nitro compounds (ANC). A clear difference was observed in the quenching efficiency between (R)- and (S)-ANC, with (R)-ANC quenching the terthienyl cellulose derivative emission in a more efficient way compared to the (S)-ANC stereoisomer. Notably, the authors reported on the importance of the helical chirality of the cellulose rather than on the central chirality in the repeating glucose units for chiral fluorescence sensing [141].

4.1.3. Colorimetry ("Naked Eye" and UV-Absorbance)

Optical visual sensors are important sensing systems as they allow for the rapid detection of analytes in screening applications. Importantly, in these systems, signal transduction is achieved by a change in color, detectable by the naked eye. In addition, color changes can be accurately referred to analyte concentration thanks to the use of image analysis software. For example, from ImageJ Photoshop software, variation in colors intensity [143] as well as variation in lightness (white to black), color ranges from red to green, and color ranges from yellow to blue [143] can be derived.

To achieve environment-responsive coloring, synthetic dyes (i.e., cresol red, bromocresol blue/green/purple, xylenol blue, etc.), natural colorants (i.e., curcumin and anthocyanin from red cabbage, black rice and purple sweet potatoes) and/or metal nanoparticles (i.e., gold, silver and platinum NPs) have been used as indicators. These chromic materials are able to reversibly change color upon an external stimulus such as light, heat, pH and exchange-processes with the analyte.

As described in the previous section, cellulose is excellent both (i) as substrate for the anchoring of chromophore and (ii) as a scaffold for nanoparticles and biomolecules embedding. For example, pH (and NH_3) sensing was achieved by anchoring red cabbage (RC) pigment into CNF [144] and carboxymethyl cellulose (CMC) [145], either alone or in composite systems. In particular, electrospun non-woven cellulose fibers (Cs-ESNW) loaded with the RC pigment (RC/Cs-ESNW) showed visibly distinct colors over a wide range of pH (Figure 8a). In other examples, colorimetric systems based on BC embedded with curcumin were developed for (i) Pb^{2+} ions detection thanks to the color change from yellow to red upon formation of the curcumin-Pb^{2+} chelation complex (Figure 8b) [146], (ii) a colorimetric metal-complexing indicator-displacement assay (M-IDA) for zoledronic acid (ZA) (Figure 8c) [147], and (iii) sensing of human serum albumin (HSA) in human blood serums due to the ability of HAS to prevent curcumin alkaline hydrolysis/degradation at low pH (Figure 8d) [148], demonstrating the versatility of these systems towards both chemo- and biosensing.

In addition, the aggregation or etching (decrease in population density of the metal NPs and increase in the interparticle distance) of embedded metal NPs into cellulose scaffolds have been exploited for optical sensing. For these systems, the use of cellulose as a scaffold can enhance sensor performance by modulating the size, shape, composition and interparticle distance of the NPs, as previously described for the SERS-based sensors. In particular, cellulose presents a 3D network with tailorable porosity, high content of hydroxyl group or other functional groups that can be used as a reducing and/or anchoring component for metal NPs synthesis and stabilization and a large specific surface area that facilitates metal NPs–analyte interaction. Among celluloses, we rationalize that CNFs and BCs better represent the properties described above due to their purity, nanoscale, fibrillar network, high spinnability and film-forming properties.
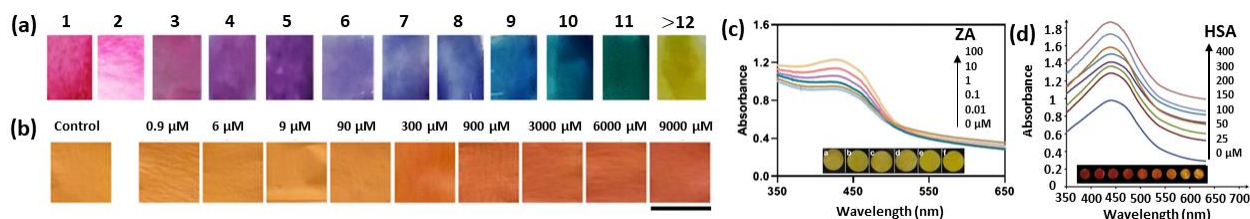
Figure 8. (**a**) Color scheme of the dyed RC/Cs-ESNW nanofiber mats, which developed different colors upon pH changes (pH 1–14), indicating that the color-changing ability of RC extract is retained after immobilization in the electrospun non-woven cellulose fiber (Cs-ESNW) matrix [144]. (**b**) Scanned images of the curcumin-embedded BC strip in the absence (control) and in the presence of different concentrations of Pb^{2+} ions (Scale bar: 0.5 cm) [146]. (**c**) Changes in absorption intensities and color (insert) of the curcumin-doped BC nano-paper coupled with Fe(III) ions (100 μM) at 427 nm with various concentrations of zoledronic acid (ZA) [147]. (**d**) UV-vis absorption spectra and photographical images (insert) of the curcumin-embedded BC nano-paper with various concentrations of HSA in the range of 0 to 400 mM [148]. Copyrights: all images have been adapted and reproduced with permission from: (**a**) © 2014 Elsevier B.V.; (**b**) © 2021, Iranian Chemical Society; (**c**) © 2019, Springer-Verlag GmbH Austria, part of Springer Nature; (**d**) © 2019 Elsevier B.V.

In the literature, there are several examples of metal NPs embedded into BCs networks. For instance, BC has been used for the formulation of NPs embedded in BC films with optical sensing capabilities. In a work reported by Morales et al., the formulation of AgNP-BC and AuNP-BC composites (Figure 9(i)) was reported for the sensing of methimazole or iodine, on one side, and thiourea or cyanide, on the other side. For these systems, the metal NPs' aggregation leads to a change in color of the NPs–BC composites towards darker shades and to a red shift in the UV-vis spectra. Specifically, the interaction between the thiol groups of methimazole and the AgNPs promoted the aggregation of particles with consequent changes in color of the AgNP–BC composite system from yellow to dark yellow. AgNPs' interaction with thiourea, instead, leads to a color change of the AuNP–BC composite system from red to dark red and to a local minimum in the UV-vis spectra in the range of 430 to 440 nm (Figure 9(ii)). Particles etching, on the contrary, was reported to cause a change in color of the NPs–BC system towards lighter shades and a concentration-dependent blue shift in the UV-vis spectrum. In particular, AgNPs' interaction with iodide cause a change of the AgNPs–BC composite from yellow to light yellow, while the interaction between AuNPs and cyanide determines a change of the AuNPs–BC composite from red to light pink (Figure 9(iii)) [121].
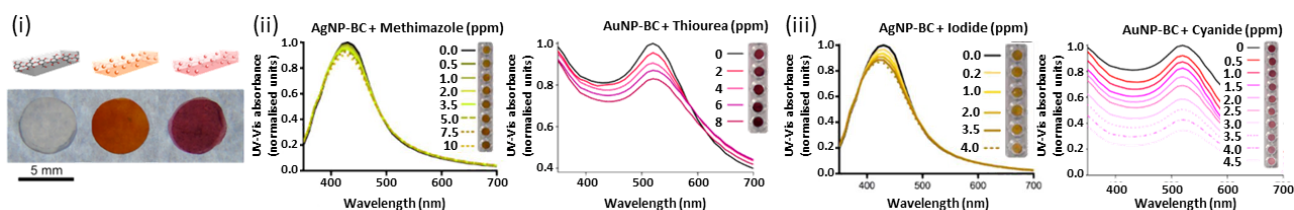

Figure 9. (i) Schematic representation (top) and photographical images of BC, AgNP–BC and AuNP–BC plasmonic nano-paper composites (from left to right). (ii) Change in UV-vis spectra and color of AgNP–BC paper composite upon addition of methimazole and of AuNP–BC upon addition of thiourea. (iii) Change in in UV-vis spectra and color of AgNP–BC upon addition of iodide and of AuNP-BC upon addition of cyanide [121]. Copyrights: all the images have been adapted and reproduced with permission from © 2015, American Chemical Society.

In another example, Teodoro et al. developed a colorimetric sensor based on a AgNPs–CNC composite, which displayed high sensitivity (detection limits of 0.014 μM) and selectivity (no interference with Cu^{2+}, Zn^{2+}, Fe^{2+}, uric acid and glucose) toward H_2O_2 detection in water and milk matrices. In this system, a decrease in the AgNP absorption

band at 410 nm together with a color change from yellow to colorless was caused by the catalytic decomposition of AgNPs at increasing concentrations of H_2O_2 [149].

Recently, the use of carboxymethyl cellulose (CMC) as a scaffold for the performance of a nanozyme (Prussian blue nanoparticles, PB NPs)–enzyme (glucose oxidase, GOx) cascade reaction in the colorimetric detection of glucose has been reported (Figure 10(i,ii)) [150]. In this system, CMC plays multiple roles as it acts (i) as a capping agent for the synthesis, immobilization and protection from coalescence of PB NPs, (ii) as a biocompatible polymer due to its ability to preserve GOx activity, (iii) as a compartmentalizing agent which confines the integrated enzyme–nanozyme system in proximity, favoring in this way the cascade reactions (Figure 10(iii)), and (iv) as a protective agent for the nonspecific adsorption of biomacromolecules (i.e., serum proteins from complex biological samples) on the nanozyme surface. The sensing strategy in the developed biosensor relied on the catalytic oxidation of glucose by GOx into H_2O_2, and in the subsequent catalytic reduction in H_2O_2 by the PB NPs in the presence of ABTS (chromophore), which resulted in the formation of the dark green $ABTS^{\bullet+}$ product, detectable at 420 nm [150].
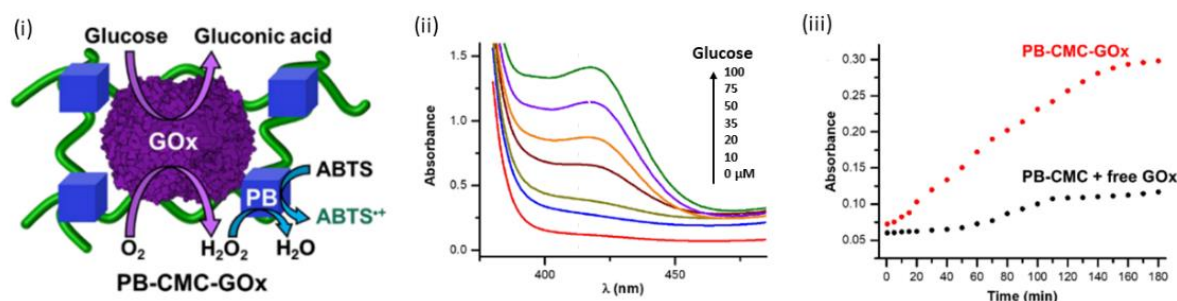

Figure 10. (i) Schematic representation of the integrated system composed of glucose oxidase (GOx) and Prussian blue nanoparticles (PB NPs) embedded within a CMC-based hydrogel (GOx-PB–CMC) and the catalyzed cascade reactions for the detection of glucose. (ii) UV-vis spectra of the $ABTS^{\bullet+}$ oxidation reaction upon addition of different concentrations of glucose and (iii) comparison of the catalytic reaction rate of PB–CMC–GOx integrated system (red curve) and of PB–CMC composites with free GOx added in solution (black dots) upon addition of 20 μM glucose, highlighting the proximity effect that cellulose operates by confining GOx and PB NPs [150]. Copyrights: all the images have been adapted and reproduced with permission from © 2022, Baretta et al., published by American Chemical Society.

Cellulose paper is a promising material for catalysts and enzymes support, as it provides unique geometry and hydrophilic/hydrophobic balance [151]. For these reasons, in recent times, cellulose filters or chromatography papers have been on the focus as biocompatible and inexpensive materials, ideal for enzymes immobilization. In particular, cellulose-paper fine fiber matrix, together with its inherent hydrophilicity, provides an excellent biocompatible microenvironment for the preservation of the enzymes' catalytic activity [152]. In addition, the introduction of hydrophobic functionalization on cellulose surface allows for the efficient absorption and immobilization of the enzymes due to the hydrophobic interactions [153]. For example, a paper-based colorimetric biosensor based on phenylalanine ammonia lyase (PAL) hybrid nanoflowers was proved to semi-quantitatively detect the concentration of phenylalanine from urine samples with a good linearity to the phenylalanine concentrations (60 to 2400 μM) and a response time of only about 10 min [154].

A particular case of naked-eye sensors based on cellulose is the one of CNC, which is able to form photonic films by solvent-evaporation-driven self-assembly. Indeed, given its chiral nematic structure, CNC films can reveal distinct colors without the use of chromophores. These films can undergo color change on the bases of the chiral nematic step (helix pitch) and on the CNC pseudoplanes interspaces. For these reasons, CNC films have been used for humidity sensing, with a change in color driven by water absorption

when exposed to environments with high relative humidity [92]. For example, the work reported by Bumbudsanpharoke et al. showed a color switch from pink to bluish (shift of 160 nm towards longer wavelengths) in a film composed by NaCl and CNC upon moisture absorption [14,155]. Besides moisture detection, the same adsorption principle has been used for the detection of volatile inorganic and organic compounds. For example, Shidong et al. reported on a detection system of ammonia based on CNC films doped with Cu^{2+}. In this case, Cu^{2+} was used as a color tuning agent given the strong chelation between the metal and the negatively charged CNC [156]. Song et al. on the contrary, managed to obtain CNC films with different color patterns by the selection of the films' thickness and by aiding the close packing of CNCs with 1-butyl-3-methylimidazolium, an ionic liquid able to screen the repelling electrostatic charges between CNCs. The introduction of amine groups into the films allowed for the visual detection of formaldehyde and propanal gases without interference from other molecules [157]. Finally, reversible stimuli-responsive stretchable optics based on CNC were obtained by embedding an elastomer into a CNC network (Figure 11). Indeed, the mechanically induced switch between the CNCs chiral nematic and pseudo-nematic arrangement determines the appearance/disappearance of a vivid interference color [158].
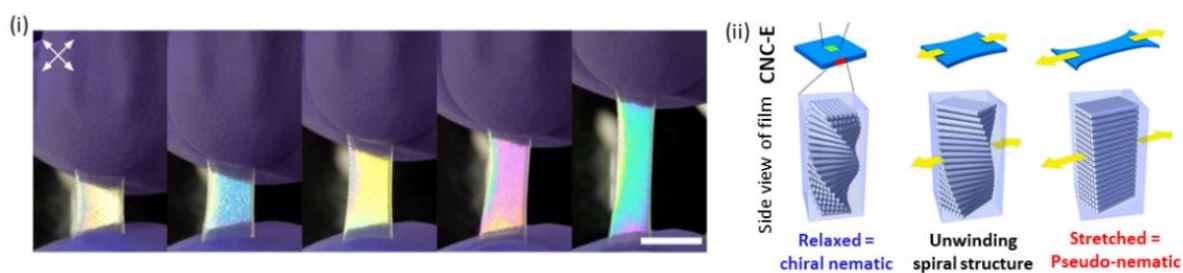

Figure 11. Photographs of CNC-E stretching viewed under crossed polarizers (i), with color changes from white to blue to yellow to pink to green upon stretching, and (ii) schematic illustration of reorientation of CNCs from chiral nematic to a pseudo-nematic structure as the film is stretched [158]. Copyrights: all the images have been adapted and reproduced with permission from © 2019, Osamu Kose et al. published by Springer Nature.

4.1.4. Cellulose-Based Lateral Flow Assays (LFA)

Optical sensing strategies combined with portable and easy-to-handle devices are pivotal for the easy, fast and accurate detection of an analyte at points of care (POCs) for diagnosis purposes or for environmental and agro-food safety monitoring, among others. Lateral flow assays (LFAs) tests are the hallmark of portable and disposable devices. LFAs are composed by a supporting and adhesive backing card or a plastic housing where a sample pad, a conjugate release pad, an analytical strip and an absorbent pad are mounted. The liquid sample is introduced into the sample pad and mixed with the reagents needed for the test in the release pad; it then flows through the analytical strip, where the signals are generated and detected, and finally ends up in the absorbent pad which acts as a sink. The analytical strip is of particular importance as it involves critical steps in the LFAs: (i) the formation of the immunocomplexes and (ii) the visualization of the LFAs response.

In conventional LFAs, the analytical strip is typically made of porous nitrocellulose (NC) membranes/films casted to reach a thickness of about 100 to 150 μm [159]. These films are usually mixed with surfactants to moderate the natural hydrophobicity of NC and improve its wettability and capillary flow rate. Thanks to its inherent hydrophobicity, NC is able to establish both hydrophobic and hydrogen bond interactions with proteins, which translates into a high protein immobilization capability. For example, it was reported that NC absorbs more than 100 μg of IgG per cm^2 [159]. However, since protein molecules absorb almost instantaneously in NC, a blocking step, such as saturation of NC with BSA, is required to allow for the flow of the protein in the tested sample [160]. Additional advantages of the use of NC are its wide range of pore size and porosity, its brightness

and its competitive price. Nonetheless, NC also presents some shortcoming for LFAs development. First, the inherent brittleness of NC makes it difficult to formulate and handle unbacked membranes. To overcome this issue, the casting of NC onto polyester films was proven to be an effective way to produce a handling membrane as NC does not easily delaminate from polyester. In addition, NC presents high sensitivity to humidity, flammability and lot-to-lot analytical reproducibility variability. Finally, the interaction with proteins via absorption indicates an inherent inability to present the receptor at a precise and correct orientation, with a consequent loss in recognition activity and a need to use an excess of proteins. For these reasons, alternatives to the NC analytical strip have appeared in the literature, with a high focus on the use of paper. For example, the ability to use paper from different sources (acacia, birch, eucalyptus and spruce) and different chemical treatment hardness (bleaching) and the addition of other cellulose derivatives, such as CMC, to improve handling has been tested [160]. In particular, 80 g/m^2 of paper made of unbeaten, bleached eucalyptus pulp with a dosage of 2.5 g/kg PAE (a wet strength additive) as a membrane material for a noncompetitive immunoassay test for hemoglobin and morphine was demonstrated [160,161]. Nonetheless, this work also demonstrates how the variability of the paper's physical properties (i.e., brightness, wet strength and lateral flow speed) is predominantly determined by the source of the native fiber and by how the fibers and fibrous network are modified and treated during the papermaking, which can be an issue for analytical reproducibility [160]. However, these works represent a pivotal step forward in the use of cellulose not just in the sample and absorbent pads, as conventionally done, but also in the formulation of analytical strips.

Besides its role as LFAs support membrane, the use of cellulose to enhance LFAs sensitivity has recently been reported. LFAs sensitivity is commonly related to the paper porosity, with smaller pores correlating with a higher sensitivity. Nonetheless, a general reduction in pore size along the analytical strip can lead to difficulties in flow. To prevent this, the layering of cellulose nanofibers (CNFs) only at the test line area of the NC strips has been proposed. This modification leads to a higher concentration of bioreceptors in the strip surface, which translates into an increased density of selectively attached gold nanoparticles (AuNPs), resulting in an average boost of 36.6% in sensitivity for IgG detection [162].

Recently, Natarajan et al. proposed to combine the use of commercially available cellulose filter paper as LFA analytical strip with the use of CNF for sensitivity enhancement, demonstrating the feasibility of replacing an NC-based analytical strip with standard cellulose paper filter (chromatography paper Whatman N.1) without loss in LFAs performance [163]. The efficiency of developed LFAs was tested for the quantitative detection of cardiac troponin I (cTnI), with detection and quantitation limits equivalent to those reported for standard NC LFA (1.28–1.40 ng/mL and 2.10–2.75 ng/mL for LFAs with cellulose and cellulose CNF strips, respectively).

4.1.5. Cellulose for Surface Plasmon Resonance (SPR) Immunosensing

Surface plasmon resonance (SPR) is a surface spectroscopic technique that allows the label-free detection of the analyte–receptor binding event. Briefly, the interaction between an electromagnetic wave under suitable conditions and the free electrons at the interface of a thin metal, typically gold, and a dielectric medium leads to collective charge (electron) oscillations. The reflectivity is measured as a function of the incident angle of the light on the thin gold layer. The resonance condition, which determines the excitation of these surface plasmons (surface plasmon resonance, SPR), results in a dip in the reflected light at a specific angle. Following a binding event between a receptor, immobilized on the gold surface, and the analyte, introduced by a flowing solution, a change of the curve reflectivity versus incident light is measured.

Originally, receptors (usually antibodies) are immobilized on the gold surface, previously functionalized with self-assembled monolayers (SAMs), in order to prepare a layer of antibody on the gold surface [164,165], even though this approach results in low sensitivity and specificity of the SPR immunosensor [166]. An alternative approach involves the use

of 3D hydrogel coating for the immobilization of the antibody on the gold surface. In this regard, cellulose has been demonstrated to be an exceptional material for the fabrication of SPR immunosensors interface.

In particular, given its ease in functionalization and wide processability, cellulose can form films/membrane with tailored porosity (as in the case of cellulose acetate), which is particularly important in SPR analysis as it makes it possible to monitor the binding of the analyte on the multilayers immobilized antibody with high sensitivity [167]. Importantly, the use of acetate cellulose and nitro cellulose was also reported for their capillary flow-inducing properties [167]. In particular, biosensors based on cellulose derivatives have been developed for the detection of human IgG using immobilized anti-human IgG (produced in goats) from non-homogenized milk; the authors demonstrated the ability of the biosensor surface functionalized with a cellulose membrane to prevent the interference with the fat globules, which are highly concentrated in non-homogenized milk [167]. In this study, anti-human IgG was immobilized on the cellulose surface by a spontaneous adsorption process. Even though protein surface adsorption has been widely used for the formation of immunoassays, current limitations such as adsorption in regions not accessible to the antigen or desorption processes must be tackled. In this regard, the formulation of cellulose into soft cellulose II nanospheres (NPcat) adsorbed on ultrathin films of CNF was reported as a strategy to form colloidal nanogels with a remarkably enhanced protein affinity, as demonstrated by the improved nonspecific (BSA) and specific (human immunoglobulin G) protein adsorption [108].

Carboxylated cellulose derivatives, such as TEMPO-oxidized cellulose or carboxymethyl cellulose (CMC), have been reported to directly conjugate antibodies by amide coupling, preventing in this way desorption processes [5,57]. Importantly, the SPR immunosensors' performance is highly dependent on the ability of the analyte (antigen) to bind the immobilized antibody. In this regard, the stability of the protein folding is sometimes hindered by a chemical conjugation, which can result in up to 50% of loss of the recognition ability. In order to prevent this shortcoming, the concomitant adsorption of the protein-grafting polymer into another cellulose surface has been proposed, in a process defined as assisted conjugation. For example, in a work reported by Orelma et al. [5], the functionalization of a cellulose model surface by the irreversible adsorption of CMC, followed by the covalent linking of anti-hemoglobin antibodies to CMC was proposed. The resulting biointerface allowed for the detection of hemoglobin with an LOD of 0.1 μg/mL.

In addition to its anchoring properties, CMC has been demonstrated to reduce nonspecific interactions with other proteins (antifouling) in a comparable manner to poly (ethylene glycol) (PEG). This property has been attributed to the ability of CMC to create a protective layer composed of tails and loops due to its ability to swell and to form a highly hydrated layer [5]. The prevention of non-specific adsorption of proteins from complex samples is fundamental to develop reliable sensing interfaces.

Anionic carboxylated cellulose derivatives are not the only suitable candidates for the formation of bioconjugates. Indeed, another class of cellulose derivatives, aminocelluloses, have been reported to effectively graft and stabilize oxidoreductases enzymes—glucose oxidase (GOx), horseradish peroxidase (HRP) and lactate oxidase (LOD)—with different coupling strategies [3,168–170]. Importantly, the presence of amino functional groups on cellulose surface, as well as its demonstrated biocompatibility, opens the venue for the use of aminocellulose for oriented antibody immobilization [171].

4.2. Cellulose in Electromechanical, Electrochemical and Opto-Electronic (Bio)Sensing

Electromechanical and electrochemical sensors based on cellulose have been largely employed for the detection of various analyte and environmental stimulus. Electromechanical sensors translate pressure and/or strain into variations of electrical properties measured as increase/decrease in electrical current, changes in electrical voltage and/or changes in the systems resistance. In electrochemical sensing, instead, the signal is generated by the electrochemical reduction/oxidation of the analyte directly (electroactive species) or

indirectly. Importantly, both transduction methods are highly sensitive, selective, simple, stable and cost effective [14]. In addition, opto-electronic sensors are able to couple electrochemical response (like current intensity) with optic properties (like absorption or emission). These hybrid sensors overcome the shortcoming of the two detection techniques alone, improving the analytical performances [172].

For these transduction techniques, the choice of the material for either the fabrication of the electrode or its surface modification is pivotal. Indeed, electrode surfaces are generally modified with different nanomaterials (i.e., metal nanoparticles or carbon-based nanomaterials such as CNTs or graphene) to enhance their sensing threshold and response by improving their electrical conductivity, specificity or electrocatalytic properties. These nanomaterials are usually embedded into a polymeric matrix with which the electrode is coated. Specifically, coating materials directly affect the electrode-specific surface area and the immobilization of the receptor (and, in turn, its interaction with the analyte) as well as the sensor sensitivity, specificity and detection limit. Thanks to its physicochemical properties, cellulose is a very promising material for electrode modification, despite its inherent nonconductivity. In fact, substantial efforts have been made towards the development of cellulose-based electrical sensing devices. In short, cellulose applicability for electrode modification falls into its hydrophilicity, high aspect ratio and large surface area, high presence of hydroxyl group for biomolecules functionalization, 3D network and film-forming ability, tailorable porosity, thermal stability and good mechanical and optical properties [173].

Besides the use of cellulose in electrode modification, a new class of functional material, called nanomaterial-modified conductive cellulose (CP) has recently emerged. CP found application in the development of wearable, lightweight and portable POCs devices. Indeed, paper has been demonstrated to present competitive properties for POCs electrical devices due to (i) the high surface-to-volume ratio, which allows for the storage of reagents in high amounts, (ii) the mesoporous structure, in which electrolytes and ions can diffuse and (iii) the stability in electrochemical and mechanical performances. For further information about CP and its application, we refer the reader to the topic-specific review recently published by Kumar et al. [174].

4.2.1. Electromechanical Sensing

Regarding electromechanical sensing, cellulose-based substrates have found several applications in strain, pressure and even proximity sensing. For these systems, the detection is based on a change in the system conductivity and relative resistance under an applied mechanical input. For these types of sensors, a well-connected conductive network exists in the initial state. Under application of tensile force, slippage creates discontinuities in the conductive network which translates into an increased resistance. Under compressive force, instead, the increased contact between the conductive network translates into a decreased resistance.

For example, an anti-freezing and conductive cellulose-based hydrogel with strain-sensing properties has been developed by Chen et al. [175]. Briefly, hydroxypropyl methylcellulose (HPMC) was dissolved in an aqueous zinc chloride solution and grafted with acrylonitrile and acrylamide copolymers (HPMC-g-AN/AM-ZnCl$_2$) using ceric ammonium nitrate as initiator. The obtained hydrogels showed ultra-stretchability (1730%), excellent tensile strength (160 kPa), high elasticity (90%), good toughness (1074.7 kJ/m^3), fatigue resistance, as well as electric conductivity (1.54 S/m) and anti-freezing performance (−33 °C). In particular, the ion mobility in the hydrogel matrix, together with the dispersion of metal ions in the cellulose medium, were attributed to the hydrogel's good electrical conductivity. Additionally, the hydrogel exhibited changes in conductivity, measured as the relative variation of resistance, upon application of different strains (Figure 12a). In particular, for this system, compression strain and tensile strain both resulted in an increase in conductive resistance due to the narrowing of the water molecule channels and increase impedance in ions movement [175].
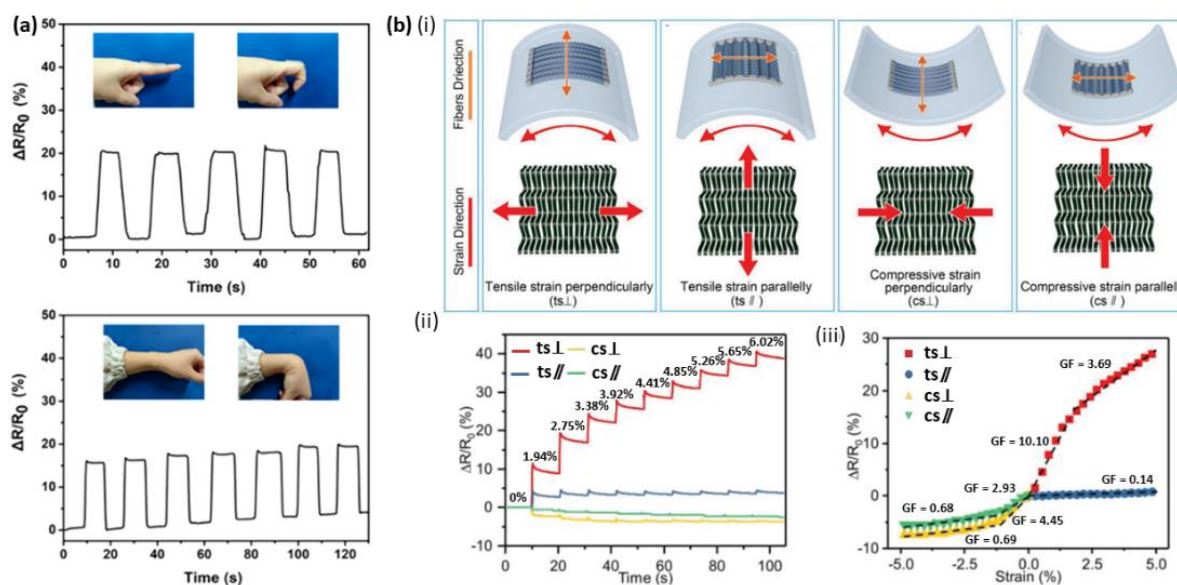
Figure 12. (**a**) Change in the HPMC-g-AN/AM-ZnCl₂ hydrogel sensor relative resistance upon finger (top) and wrist (bottom) bend/stretching, respectively [175]. (**b**) Sketch of the four different bending modes of the flexible cellulose-based carbonized crepe paper (CCP) strain sensor (i): tensile strain perpendicularly (ts⊥), tensile strain parallelly (ts∥), compressive strain perpendicularly (cs⊥) and compressive strain parallelly (cs∥) as well as the relative resistance change under various bending strains (ii) and the relative resistance change as a function of strain (iii) [176]. Copyrights: all the images have been adapted and reproduced with permission from: (**a**) © 2020, American Chemical Society; (**b**) © 2018 WILEY-VCH Verlag GmbH & Co., KGaA, Weinheim.

A particular application of cellulose is given by its inherent anisotropy, which has been translated into a strain sensor able to respond differently to forces applied parallel or perpendicular to the aligned cellulose chains. In particular, thermal treatment under N₂ atmosphere converted the nonconductive crepe cellulose paper into a conductive carbon fiber network while retaining its original anisotropic structure (Figure 12b). Hence, the obtained carbonized crepe paper (CCP) showed high flexibility, fast response (<115 ms), high durability (10,000 cycles), negligible hysteresis and, in particular, extremely different gauge factors (GFs) in bending perpendicular and parallel to the fiber direction. In addition, the application of the developed system in detecting complex human motions and controlling a 2-degree-of-freedom robot arm as a wearable device have been demonstrated [176].

In a work reported by the research group of Ikkala, the combination of CNFs with few-walled carbon nanotubes (FWCNTs), both in aerogel form, led to the formation of a mechanoresponsive pressure-sensing system, which appeared to have different performance (conductivity and relative resistance) based on the composite system morphology. In fact, the investigated systems presented a sheet-like or a fibrillar structure based on the freezer-drying process (with liquid nitrogen or with liquid propane, respectively) [177].

In another work, CNC grafted with reduced graphene oxide (GOr–CNC) showed proximity sensing, as demonstrated by the measurement of current-voltage-resistance of the sample. GOr–CNC was reported to be a non-linear semiconductive material with a lower current in comparison to GOr alone. In particular, the increase in resistance and, in turn, the decrease in conductivity was attributed to the CNCs' ability to create a hole-depletion region near the interface with the reduced GOs, hence the interference of CNCs on GOr network [178].

4.2.2. Electrochemical (Bio)Sensing

In electrochemical sensing, the interaction of an analyte and its receptor in an electrolyte solution is usually transduced by potentiometry and amperometry. Common problems associated with electrochemical detection, which can hinder their applications

in real (clinical and environmental) samples, are fouling (i.e., adsorption of large organic surfactants, proteins or reaction products to the electrode surface) and selectivity. Importantly, cellulose has been demonstrated to be an ideal membrane to overcome the mentioned issues.

For example, cellulose acetate was shown to have both antifouling and permselective properties; the first thanks to its ability to form a barrier against organic surfactants transport [179], the second thanks to its tailorable permeability, controlled by different time periods of the alkaline hydrolysis [180]. Hence, electrodes modified by cellulose acetate have shown increased stability and selectivity in the anodic stripping of trace metals [181], the amperometric detection of organic compounds [182] and in the selective detection of ionic neurotransmitters [180].

Besides its antifouling and permselective properties, cellulose has been employed as a solubilizing agent. For example, the hydrophilic nature of some cellulose derivatives (methyl cellulose, hydroxypropyl cellulose, hydroxypropyl methyl cellulose, carboxymethyl cellulose) has been used to solubilize water insoluble macromolecules, such as poly-aniline (PAni) for hydrazine detection [183]. Aniline monomers were grafted on methyl cellulose, hydroxypropyl cellulose and hydroxypropyl methyl cellulose chains (MC, HPC and HPMC) and then polymerized by addition of ammonium persulfate APS as an oxidation initiator, resulting in PAni-cellulose derivatives with hydrazine-sensing capabilities [183]. The authors compared the sensitivity enhancement obtained by the use of these different types of cellulose derivatives, attributing the best sensitivity of 0.0143 ppm^{-1} reported for PAni-MC to the less steric hindrance effect by the methyl substituents in MC. In another example, a gas sensor based on PAni nanorods was prepared via a co-doping method with 5-sulfosalicyl acid (SSA) and poly(2-acrylamido-2-methyl-1-propane sulfonic acid) (PAMS) on a bacterial cellulose substrate [184].

In recent years, the combination of cellulose with carbon nanomaterials, such as graphene [185], graphene oxide (GO) [186], single-walled carbon nanotubes (SWCNT) [187], multi-walled carbon nanotubes (MWCNTS) [188] and nanodiamonds [189], has emerged as a promising strategy to prepare nanocomposite materials for different electrochemical applications, including amperometric sensing. Transparent, ultrastrong and printable conductive nanocomposites have been obtained from the combination of 2,2,6,6-tetramethylpiperidine-1-oxyl (TEMPO)-oxidized cellulose nanofibrils (TOCNFs) with SWCNTs [187]. A recent study addressed the stability of four different nanocomposites comprising fibrillar nanocellulosic materials with different functional groups (sulfate, carboxylate and amino-silane) and MWCNTs. The investigated nanocomposites showed an excellent stability over a wide potential range (-0.6 to +1 V) and in different electrolytes [188]. Owing to the excellent electrochemical properties, various nanocomposites comprising nanocelluloses and MWCNTs or SWCNTs have been proposed as electrode materials for the amperometric detection of biomolecules. For example, a composite membrane assembled from MWCNTs and sulfated nanofibrillar cellulose (SNFC) has been employed for the selective and sensitive detection of dopamine at nanomolar concentrations (LOD of 65 nM) [190]. A modified electrode was successfully prepared by using a nanocellulose/MWCNTs hybrid for the detection of diclofenac in pharmaceutical products and biological fluids [191]. Differential pulse voltammetry (DPV) allowed for the determination of diclofenac on the modified electrode with a detection limit of 0.012 mM. Electrodes with large surface areas, good conductivity and high porosity were obtained from a nanocomposite made of nanocellulose and single-walled carbon nanohorns (SWCNH). The modified electrodes were employed for the simultaneous detection of guanine and adenine by linear sweep voltammetry [192].

Paper-based screen-printed electrodes modified with carbon nanotubes and ferrocene (Fc)-labelled DNA (Fc-DNA) were also developed for the detection of microRNAs (miRNAs) in serum samples (Figure 13) [193]. The combination of DNA on paper-based modified electrodes leads to high stability and sensitivity of the bioassay, holding great potential for point-of-care (POC) diagnosis. Recently, a composite paper made of cellulose fibers, carbon fibers (CFs, which confers conductivity), and graphene oxide (GO, which con-

fers electrocatalytic activities) was prepared by adapting a conventional papermaking method [194]. This large-scale approach allows for the fabrication of low cost, high-performance paper-based electrochemical sensors. Indeed, the composite paper showed stable and reproducible electrochemical properties and provided electrocatalytic activities for the development of sensitive amperometric sensors.
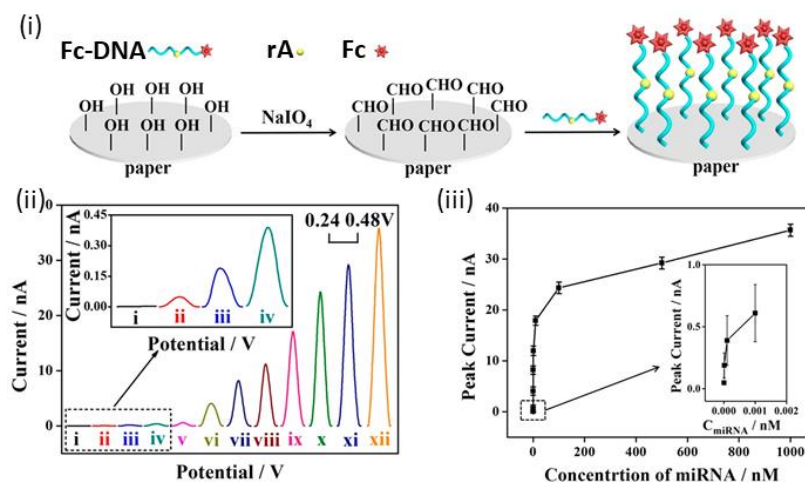

Figure 13. Preparation of paper-based electrochemical sensing platform for miRNA based on the immobilization of ferrocene (Fc)-labeled DNA (Fc-DNA) on paper (i). Detection of the lung cancer-specific biomarker miRNA-21 at different concentrations by differential pulse voltammetry (DPV) (ii) and the corresponding calibration curve (iii) [193]. Copyrights: all images have been adapted and reproduced with permission from © 2019, American Chemical Society.

Finally, thanks to its inherent chirality, 2,2,6,6-tetramethylpiperidine-1-oxyl (TEMPO)-oxidized cellulose nanocrystals (TOCNCs) was used as a coating agent of a L-cystine (L-Cys)-modified Au electrode for the design of a novel enantioselective electrochemical sensor. In this case, in which cellulose acts as an enantio-selective receptor, TOCNC expressed weaker interaction with L-amino acids than with D-amino acids, resulting in a higher peak current in cyclic voltammetry (CV) and differential pulse voltammetry (DPV) [195].

4.2.3. Optoelectronic (Bio)Sensing

Optoelectronic sensing devices, hybrid systems with coupled optical and electrochemical transduction, require an electrode substrate with high transparency for optical detection and good electrocatalytic activity/conductivity for electrochemical detection. In this context, cellulose is an ideal material for the formulation of highly transparent, mechanically competitive, biocompatible membranes able to finely disperse a variety of nanomaterials, such as indium tin oxide, graphene, carbon nanotubes and/or metallic nanowires. Among these, metallic nanowires (especially Ag NWs), which are particularly promising for application in flexible electronic devices, have shown better adhesion to cellulose [196] in comparison to other conventional transparent flexible substrates [197]. For example, a regenerated cotton cellulose transparent film was spray-coated with Ag NWs and its performance under stretching and bending (strain sensor) was evaluated by measuring the sheet resistance variation in the Ag NW transparent film. Interestingly, UV-visible transmittance measured in the range of 200–800 nm shows an absorption band between 300 and 400 nm, whose intensity increases upon increase in Ag NWs concentration. Nonetheless, no studies about changes in the transmittance intensity or wavelength upon application of strain were reported [196].

Recently, nanocelluloses, thanks to their exceptional mechanical and optical properties, have also found applications in optoelectronic devices. In particular, fibrillar nanocelluloses, CNFs and BCs, have been reported to form highly transparent and mechanically

competitive films. For example, an electro-opto-mechanical sensing device composed by CNF and ZnO has been developed by Zhai et al. [198]. In this work, TEMPO-oxidized CNFs films embedded with ZnO showed a lowest transparency of 80% in the visible light range for 50 mM of ZnO and piezoelectric properties upon strain application, attributed to the dipolar orientation between the ZnO nanorods and the CNF film surface. In addition, the generation of induced current outputs under UV irradiance was reported. Interestingly, a higher current output was generated when the cellulose side was exposed to radiation (3 mW/cm^2), in comparison with the ZnO nanorods side, an effect which is attributed to a lower scattering of the UV irradiance from cellulose [198].

In another example, a transparent film of BCs was used as a coating membrane in screen-printed electrodes (SPE). In particular, Prussian blue was used as a probe for the opto-electrochemical detection of acetaminophen. The sensing mechanism involves electron transfer from acetaminophen (reducing agent) to Fe^{3+}. The hence formed Fe^{2+} reacts with ferricyanide to form PB, with a consequent change of color from yellow to blue and spectrophotometric absorbance at 710 nm, with the absorption peak intensity proportional to acetaminophen concentration in the range of 20–100 μM and a limit of detection (LOD) of 5.4 μM. Cyclic voltammetry analysis, instead, showed the appearance of anodic and cathodic current peaks related to the mixtures of PB/K$_3$Fe(CN)$_6$/FeCl$_3$ solutions, which gradually increased upon increase in acetaminophen concentration. The developed BC–SPE system exhibited a linear amperometric response for acetaminophen concentration ranging from 10 to 100 μM, with a good linearity (r = 0.997) and an LOD of 2.2 μM [199].

5. Conclusions and Outlook

We have reviewed the fascinating properties of cellulose and cellulose derivatives, highlighting why this material is very suitable to develop sensors and biosensors for detecting varied analytes and physical changes. In particular, some of the cellulose features can be ascribed to (i) its molecular structure and nanostructure, (ii) its long-range structural organization (i.e., the chiral nematic phase which allows for optic detection of physical changes) and high processability, as for example the formation of 3D fibril networks, nanoparticles or films, (iii) its surface functionalization, which allows for both the covalent conjugation of receptors (antibodies, enzymes, etc.) or chromophores and the establishment of supramolecular interactions for the non-covalent association with nanomaterials (e.g., metallic nanoparticles, carbon-based nanomaterials, etc.) and (iv) its high specific-surface area, which enhances the receptor–analyte interaction. In addition, cellulose is renewable, biodegradable, nontoxic, biocompatible, industrially available at low cost, thermally stable, printable and able to form highly transparent, flexible and foldable films. Given the just listed impressive features, cellulose stands out as a powerful alternative to replace petroleum-based polymers in the development of high-performance (bio)sensors.

Author Contributions: Conceptualization, V.G. and M.F.; writing—original draft preparation, V.G.; writing—review and editing, V.G. and M.F.; supervision, M.F.; project administration, M.F.; funding acquisition, M.F. All authors have read and agreed to the published version of the manuscript.

References

1. Edwards, J.V.; Prevost, N.; Sethumadhavan, K.; Ullah, A.; Condon, B. Peptide Conjugated Cellulose Nanocrystals with Sensitive Human Neutrophil Elastase Sensor Activity. *Cellulose* **2013**, *20*, 1223–1235. [CrossRef]
2. Sternberg, R.; Bindra, D.S.; Wilson, G.S.; Thévenot, D.R. Development, Covalent Enzyme Coupling on Cellulose Acetate Membranes for Glucose Sensor. *Anal. Cham.* **1988**, *60*, 2781–2786. [CrossRef] [PubMed]
3. Berlin, P.; Klemm, D.; Tiller, J.; Rieseler, R. A Novel Soluble Aminocellulose Derivative Type: Its Transparent Film-Forming Properties and Its Efficient Coupling with Enzyme Proteins for Biosensors. *Macromol. Chem. Phys.* **2000**, *201*, 2070–2082. [CrossRef]

4. Löscher, F.; Ruckstuhl, T.; Seeger, S. Ultrathin Cellulose-Based Layers for Detection of Single Antigen Molecules. *Adv. Mater.* **1998**, *10*, 1005–1009. [CrossRef]

5. Orelma, H.; Tuija, T.; Leena-Sisko, J.; Holappa, S.; Laine, J. CMC-Modified Cellulose Biointerface for Antibody Conjugation. *Biomacromolecules* **2021**, *13*, 1051–1058. [CrossRef]

6. Franco, P.; Senso, A.; Oliveros, L.; Minguillón, C. Covalently Bonded Polysaccharide Derivatives as Chiral Stationary Phases in High-Performance Liquid Chromatography. *J. Chromatogr. A* **2001**, *906*, 155–170. [CrossRef]

7. Zhang, J.H.; Xie, S.X.; Mei, Z.; Zhang, M.; He, P.G.; Yuan, L.M. Novel Inorganic Mesoporous Material with Chiral Nematic Structure Derived from Nanocrystalline Cellulose for High-Resolution Gas Chromatographic Separations. *Anal. Chem.* **2014**, *86*, 9595–9602.

8. Bledzki, A.K.; Gassan, J. Composites Reinforced with Cellulose Based Fibres. *Prog. Polym. Sci.* **1999**, *24*, 221–274. [CrossRef]

9. Golmohammadi, H.; Morales-Narváez, E.; Naghdi, T.; Merkoçi, A. Nanocellulose in Sensing and Biosensing. *Chem. Mater.* **2017**, *29*, 5426–5446. [CrossRef]

10. Lee, K.Y.; Tammelin, T.; Schulfter, K.; Kiiskinen, H.; Samela, J.; Bismarck, A. High Performance Cellulose Nanocomposites: Comparing the Reinforcing Ability of Bacterial Cellulose and Nanofibrillated Cellulose. *ACS Appl. Mater. Interfaces* **2012**, *4*, 4078–4086. [CrossRef]

11. Siqueira, G.; Bras, J.; Dufresne, A. Cellulosic Bionanocomposites: A Review of Preparation, Properties and Applications. *Polymers* **2010**, *2*, 728–765. [CrossRef]

12. Sfragano, P.S.; Laschi, S.; Palchetti, I. Sustainable Printed Electrochemical Platforms for Greener Analytics. *Front. Chem.* **2020**, *8*, 644. [CrossRef]

13. Zhao, D.; Zhu, Y.; Cheng, W.; Cheng, W.; Wu, Y.; Yu, H. Cellulose-Based Flexible Functional Materials for Emerging Intelligent Electronics. *Adv. Mater.* **2021**, *33*, 2000619. [CrossRef] [PubMed]

14. Teodoro, K.B.; Sanfelice, R.C.; Migliorini, F.L.; Pavinatto, A.; Facure, M.H.M.; Correa, D.S. A Review on the Role and Performance of Cellulose Nanomaterials in Sensors. *ACS Sens.* **2021**, *6*, 2473–2496. [CrossRef] [PubMed]

15. Payen, A. Mémoire sur la composition du tissu propre des plantes et du ligneux. *Seances Acad. Sci. A* **1838**, *7*, 1052.

16. Payen, A. Sur un Moyen D'isoler le Tissue Élémentaire des Bois. *CR Hebd. Seances Acad. Sci.* **1838**, *7*, 26.

17. Sponsler, O.L.; Dore, W.H. The Structure of Ramie Cellulose as Derived from X-ray Data. *Fourth Colloid Symp. Monogr.* **1926**, *41*, 174–202.

18. Haworth, W.N.; Hirst, E.L.; Thomas, H.A. The Existence of the Cellobiose Residue in Cellulose. *Nature* **1930**, *126*, 438. [CrossRef]

19. Staudinger, H. On Polymerization. In *A Source Book in Chemistry*; Harvard University Press: Cambridge, MA, USA, 2013; Volume 1900–1950, pp. 259–264.

20. Dieter, K.; Heublein, B.; Fink, H.P.; Bohn, A. Cellulose: Fascinating Biopolymer and Sustainable Raw Material. *Angew. Chem. Int. Ed.* **2005**, *44*, 3358–3393.

21. Kobayashi, S.; Kashiwa, K.; Kawasaki, T.; Shoda, S.I. Novel Method for Polysaccharide Synthesis Using an Enzyme: The First In Vitro Synthesis of Cellulose Via a Nonbiosynthetic Path Utilizing Cellulase as Catalyst. *J. Am. Chem. Soc.* **1991**, *113*, 3019–3084. [CrossRef]

22. Andrade, P.; Muñoz-García, J.C.; Pergolizzi, G.; Gabrielli, V.; Nepogodiev, S.A.; Iuga, D.; Fábián, L.; Nigmatullin, R.; Johns, M.A.; Harniman, R.; et al. Chemoenzymatic Synthesis of Fluorinated Cellodextrins Identifies a New Allomorph for Cellulose-Like Materials. *Chem. Eur. J.* **2021**, *27*, 1374–1382. [CrossRef] [PubMed]

23. Gabrielli, V.; Muñoz-García, J.C.; Pergolizzi, G.; Andrade, P.; Khimyak, Y.Z.; Field, R.A.; Angulo, J. Molecular Recognition of Natural and Non-Natural Substrates by Cellodextrin Phosphorylase from Ruminiclostridium Thermocellum Investigated by NMR Spectroscopy. *Chem. Eur. J.* **2021**, *27*, 15688–15698. [CrossRef] [PubMed]

24. Perez, S.; Samain, D. Structure and Engineering of Celluloses. *Adv. Carbohydr. Chem. Biochem.* **2010**, *64*, 25–116. [PubMed]

25. French, A.D.; Bertoniere, N.R.; Brown, R.M.; Chanzy, H.; Gray, D.; Hattori, K.; Glasser, W. Cellulose. In *Kirk-Othmer Encyclopedia of Chemical Technology*; John Wiley & Sons: New York, NY, USA, 2000.

26. Kadokawa, J.I.; Kaneko, K. *Engineering of Polysaccharides Materials by Phosphorylase-Catalysed Enzymatic Chain-Elongation*; Pan Stanford Publishing: Singapore, 2012.

27. Kadokawa, J.I. Precision Polysaccharide Synthesis Catalyzed by Enzymes. *Chem. Rev.* **2011**, *111*, 4308–4345. [CrossRef] [PubMed]

28. Sjöström, E. *Wood Chemistry. Fundamentals and Applications*; Academic Press: New York, NY, USA, 1981.

29. Daniel, J.R. Cellulose Structure and Properties. In *Encyclopedia of Polymer Science and Engineering*; Kroschwitz, J.I., Ed.; Wiley-Interscience Publication; John Wiley & Sons: New York, NY, USA, 1985; Volume 3, pp. 86–123.

30. Barhoum, A.; Jeevanandam, J.; Rastogi, A.; Samyn, P.; Boluk, Y.; Dufresne, A.; Danquah, M.K.; Bechelany, M. Plant Celluloses, Hemicelluloses, Lignins, and Volatile Oils for the Synthesis of Nanoparticles and Nanostructured Materials. *Nanoscale* **2020**, *12*, 22845–22890. [CrossRef]

31. Munoz-Garcia, J.C.; Corbin, K.R.; Hussain, H.; Gabrielli, V.; Koev, T.; Iuga, D.; Round, A.N.; Mikkelsen, D.; Gunning, P.A.; Warren, F.J.; et al. High Molecular Weight Mixed-Linkage Glucan as a Mechanical and Hydration Modulator of Bacterial Cellulose: Characterization by Advanced NMR Spectroscopy. *Biomacromolecules* **2019**, *20*, 4180–4190. [CrossRef]

32. Zhu, S.; Wu, Y.; Chen, Q.; Yu, Z.; Wang, C.; Jin, S.; Ding, Y.; Wu, G. Dissolution of Cellulose with Ionic Liquids and Its Application: A Mini-Review. *Green Chem.* **2006**, *8*, 325. [CrossRef]

33. Cao, X.; Ding, B.; Yu, J.; Al-Deyab, S.S. Cellulose Nanowhiskers Extracted from Tempo-Oxidized Jute Fibers. *Carbohydr. Polym.* **2012**, *90*, 1075–1080. [CrossRef]

34. Chen, P.; Yu, H.; Liu, Y.; Chen, W.; Wang, X.; Ouyang, M. Concentration Effects on the Isolation and Dynamic Rheological Behavior of Cellulose Nanofibers Via Ultrasonic Processing. *Cellulose* **2013**, *20*, 149–157. [CrossRef]

35. Romanholo, P.V.V.; Sgobbi, L.F.; Carrilho, E. Exploring Paper as a Substrate for Electrochemical Micro-Devices. *Compr. Anal. Chem.* **2020**, *89*, 1–29.

36. Heath, L.; Thielemans, W. Cellulose Nanowhisker Aerogels. *Green Chem.* **2010**, *12*, 1448–1453. [CrossRef]

37. Nishiyama, Y.; Langan, P.; Chanzy, H. Crystal Structure and Hydrogen-Bonding System in Cellulose Iβ from Synchrotron X-ray and Neutron Fiber Diffraction. *J. Am. Chem. Soc.* **2002**, *124*, 9074–9082. [CrossRef] [PubMed]

38. Nishiyama, Y.; Sugiyama, J.; Chanzy, H.; Langan, P. Crystal Structure and Hydrogen Bonding System in Cellulose Iα from Synchrotron X-ray and Neutron Fiber Diffraction. *J. Am. Chem.Soc.* **2003**, *125*, 14300–14306. [CrossRef]

39. Langan, P.; Nishiyama, Y.; Chanzy, H. X-ray Structure of Mercerized Cellulose Ii at 1 Å Resolution. *Biomacromolecules* **2001**, *2*, 410–416. [CrossRef]

40. Wada, M.; Chanzy, H.; Nishiyama, Y.; Langan, P. Cellulose IIIi Crystal Structure and Hydrogen Bonding by Synchrotron X-ray and Neutron Fiber Diffraction. *Macromolecules* **2004**, *37*, 8548–8555. [CrossRef]

41. Wada, M.; Heux, L.; Nishiyama, Y.; Langan, P. X-ray Crystallographic, Scanning Microprobe X-ray Diffraction, and Cross-Polarized/Magic Angle Spinning ^{13}C NMR Studies of the Structure of Cellulose III$_{II}$. *Biomacromolecules* **2009**, *10*, 302–309. [CrossRef] [PubMed]

42. Wada, M.; Heux, L.; Isogai, A.; Sugiyama, J. Polymorphism of Cellulose I Family: Reinvestigation of Cellulose IV$_I$. *Biomacromolecules* **2004**, *5*, 1385–1391. [CrossRef]

43. Wada, M.; Heux, L.; Isogai, A.; Nishiyama, Y.; Chanzy, H.; Sugiyama, J. Improved Structural Data of Cellulose III$_I$ Prepared in Supercritical Ammonia. *Macromolecules* **2001**, *34*, 1237–1243. [CrossRef]

44. Eichhorn, S.J.; Etale, A.; Wang, J.; Berglund, L.A.; Li, Y.; Cai, Y.; Chen, C.; Cranston, E.D.; Johns, M.A.; Fang, Z.; et al. Current International Research into Cellulose as a Functional Nanomaterial for Advanced Applications. *J. Mater.Sci.* **2022**, *57*, 5697–5767. [CrossRef]

45. Zhao, Y.; Moser, C.; Lindström, M.E.; Henriksson, G.; Li, J. Cellulose Nanofibers from Softwood, Hardwood, and Tunicate: Preparation–Structure–Film Performance Interrelation. *ACS Appl. Mater. Interfaces* **2017**, *9*, 13508–13519. [CrossRef]

46. Isogai, A.; Zhou, Y. Diverse Nanocelluloses Prepared from Tempo-Oxidized Wood Cellulose Fibers: Nanonetworks, Nanofibers, and Nanocrystals. *Curr. Opin. Solid State Mater. Sci.* **2019**, *23*, 101–106. [CrossRef]

47. Yu, H.; Qin, Z.; Liang, B.; Liu, N.; Zhou, Z.; Chen, L. Facile Extraction of Thermally Stable Cellulose Nanocrystals with a High Yield of 93% through Hydrochloric Acid Hydrolysis under Hydrothermal Conditions. *J. Mater. Chem. A* **2013**, *1*, 3938. [CrossRef]

48. Dincer, C.; Bruch, R.; Costa-Rama, E.; Fernández-Abedul, M.T.; Merkoçi, A.; Manz, A.; Urban, G.A.; Güder, F. Disposable Sensors in Diagnostics, Food, and Environmental Monitoring. *Adv. Mater* **2019**, *31*, 1806739. [CrossRef] [PubMed]

49. Peng, B.L.; Dhar, N.; Liu, H.L.; Tam, K.C. Chemistry and Applications of Nanocrystalline Cellulose and Its Derivatives: A Nanotechnology Perspective. *Can. J. Chem. Eng.* **2011**, *89*, 1191–1206. [CrossRef]

50. Medronho, B.; Lindman, B. Competing Forces During Cellulose Dissolution: From Solvents to Mechanisms. *Curr. Opin. Colloid Interface Sci.* **2014**, *19*, 32–40. [CrossRef]

51. Rowland, S.P.; Roberts, E.J.; Wade, C.P. Selective Accessibilities of Hydroxyl Groups in the Microstructure of Cotton Cellulose. *Tex. Res. J.* **1969**, *39*, 530–542. [CrossRef]

52. Chang, P.S.; Robyt, J.F. Oxidation of Primary Alcohol Groups of Naturally Occurring Polysaccharides with 2,2,6,6-Tetramethyl-1-Piperidine Oxoammonium Ion. *J. Carbohydr. Chem.* **1996**, *15*, 819–830. [CrossRef]

53. Tahiri, C.; Vignon, M.R. Tempo-Oxidation of Cellulose: Synthesis and Characterisation of Polyglucuronans. *Cellulose* **2000**, *7*, 177–188. [CrossRef]

54. Tang, H.; Butchosa, N.; Zhou, Q. A Transparent, Hazy, and Strong Macroscopic Ribbon of Oriented Cellulose Nanofibrils Bearing Poly(Ethylene Glycol). *Adv. Mater.* **2015**, *27*, 2070–2076. [CrossRef]

55. Gabrielli, V.; Missale, E.; Cattelan, M.; Pantano, M.F.; Frasconi, M. Supramolecular Modulation of the Mechanical Properties of Amino Acid-Functionalized Cellulose Nanocrystal Films. *Mater. Today Chem.* **2022**, *24*, 100886. [CrossRef]

56. Barazzouk, S.; Daneault, C. Amino Acid and Peptide Immobilization on Oxidized Nanocellulose: Spectroscopic Characterization. *Nanomaterials* **2012**, *2*, 187–205. [CrossRef] [PubMed]

57. Orelma, H.; Filpponen, I.; Johansson, L.S.; Österberg, M.; Rojas, O.J.; Laine, J. Surface Functionalized Nanofibrillar Cellulose (Nfc) Film as a Platform for Immunoassays and Diagnostics. *Biointerphases* **2012**, *7*, 61. [CrossRef] [PubMed]

58. Perlin, A.S. Glycol-Cleavage Oxidation. *Adv. Carbohydr. Chem. Biochem.* **2006**, *60*, 183–250. [PubMed]

59. Gupta, K.C.; Sahoo, S.; Khandekar, K. Graft Copolymerization of Ethyl Acrylate onto Cellulose Using Ceric Ammonium Nitrate as Initiator in Aqueous Medium. *Biomacromolecules* **2002**, *3*, 1087–1094. [CrossRef]

60. Kim, U.J.; Kuga, S. Reactive Interaction of Aromatic Amines with Dialdehyde Cellulose Gel. *Cellulose* **2000**, *7*, 287–297. [CrossRef]

61. O'Neill, E.C.; Pergolizzi, G.; Stevenson, C.E.M.; Lawson, D.M.; Nepogodiev, S.A.; Field, R.A. Cellodextrin Phosphorylase from Ruminiclostridium Thermocellum: X-ray Crystal Structure and Substrate Specificity Analysis. *Carbohydr. Res.* **2017**, *451*, 118–132. [CrossRef]

62. Yu, Y.; Tyrikos-Ergas, T.; Zhu, Y.; Fittolani, G.; Bordoni, V.; Singhal, A.; Fair, R.J.; Grafmüller, A.; Seeberger, P.H.; Delbianco, M. Systematic Hydrogen-Bond Manipulations to Establish Polysaccharide Structure–Property Correlations. *Angew. Chem. Int. Ed.* **2019**, *131*, 13261–13266. [CrossRef]

63. Wu, Q.; Meng, Y.; Wang, S.; Li, Y.; Fu, S.; Ma, L.; Harper, D. Rheological Behavior of Cellulose Nanocrystal Suspension: Influence of Concentration and Aspect Ratio. *J. Appl. Polym. Sci.* **2014**, *131*, 40525–40532. [CrossRef]

64. Chen, W.; Yu, H.; Li, Q.; Liu, Y.; Li, J. Ultralight and Highly Flexible Aerogels with Long Cellulose I Nanofibers. *Soft Matter* **2011**, *7*, 10360–10368. [CrossRef]

65. Aulin, C.; Gällstedt, M.; Lindström, T. Oxygen and Oil Barrier Properties of Microfibrillated Cellulose Films and Coatings. *Cellulose* **2010**, *17*, 559–574. [CrossRef]

66. Hornig, S.; Heinze, T. Efficient Approach to Design Stable Water-Dispersible Nanoparticles of Hydrophobic Cellulose Esters. *Biomacromolecules* **2008**, *9*, 1487–1492. [CrossRef]

67. Son, W.K.; Youk, J.H.; Park, W.H. Preparation of Ultrafine Oxidized Cellulose Mats Via Electrospinning. *Biomacromolecules* **2004**, *5*, 197–201. [CrossRef] [PubMed]

68. Gabrielli, V.; Kuraite, A.; da Silva, M.A.; Edler, K.J.; Angulo, J.; Nepravishta, R.; Muñoz-García, J.C.; Khimyak, Y.Z. Spin Diffusion Transfer Difference (SDTD) NMR: An Advanced Method for the Characterisation of Water Structuration within Particle Networks. *J. Colloid Interface Sci.* **2021**, *594*, 217–227. [CrossRef] [PubMed]

69. Schmitt, J.; Calabrese, V.; da Silva, M.A.; Lindhoud, S.; Alfredsson, V.; Scott, J.L.; Edler, K.J. Tempo-Oxidised Cellulose Nanofibrils; Probing the Mechanisms of Gelation Via Small Angle X-ray Scattering. *Phys. Chem. Chem. Phys.* **2018**, *20*, 16012–16020. [CrossRef] [PubMed]

70. Fall, A.B.; Lindström, S.B.; Sundman, O.; Ödberg, L.; Wågberg, L. Colloidal Stability of Aqueous Nanofibrillated Cellulose Dispersions. *Langmuir* **2011**, *27*, 11332–11338. [CrossRef] [PubMed]

71. McKee, J.R.; Hietala, S.; Seitsonen, J.; Laine, J.; Kontturi, E.; Ikkala, O. Thermoresponsive Nanocellulose Hydrogels with Tunable Mechanical Properties. *ACS Macro Lett.* **2014**, *3*, 266–270. [CrossRef]

72. Chau, M.; Sriskandha, S.E.; Pichugin, D.; Thérien-Aubin, H.; Nykypanchuk, D.; Chauve, G.; Méthot, M.; Bouchard, J.; Gang, O.; Kumacheva, E. Ion-Mediated Gelation of Aqueous Suspensions of Cellulose Nanocrystals. *Biomacromolecules* **2015**, *16*, 2455–2462. [CrossRef]

73. Silva, S.M.C.; Antunes, F.E.; Sousa, J.J.S.; Valente, A.J.M.; Pais, A.A. New Insights on the Interaction between Hydroxypropyl-methyl Cellulose and Sodium Dodecyl Sulfate. *Carbohydr. Polym.* **2011**, *86*, 35–44. [CrossRef]

74. Da Silva, M.A.; Calabrese, V.; Schmitt, J.; Celebi, D.; Scott, J.L.; Edler, K.J. Alcohol Induced Gelation of Tempo-Oxidized Cellulose Nanofibril Dispersions. *Soft Matter* **2018**, *14*, 9243–9249. [CrossRef]

75. Gabrielli, V.; Baretta, R.; Pilot, R.; Ferrarini, A.; Frasconi, M. Insights into the Gelation Mechanism of Metal-Coordinated Hydrogels by Paramagnetic NMR Spectroscopy and Molecular Dynamics. *Macromolecules* **2022**, *55*, 450–461. [CrossRef]

76. Fu, L.H.; Qi, C.; Ma, M.G.; Wan, P. Multifunctional Cellulose-Based Hydrogels for Biomedical Applications. *J. Mater. Chem. B* **2019**, *7*, 1541–1562. [CrossRef] [PubMed]

77. Pierre, A.C.; Pajonk, G.M. Chemistry of Aerogels and Their Applications. *Chem. Rev.* **2002**, *102*, 4243–4266. [CrossRef] [PubMed]

78. Gavillon, R.; Budtova, T. Aerocellulose: New Highly Porous Cellulose Prepared from Cellulose-NaOH Aqueous Solutions. *Biomacromolecules* **2008**, *9*, 269–277. [CrossRef]

79. Pääkkö, M.; Vapaavuori, J.; Silvennoinen, R.; Kosonen, H.; Ankerfors, M.; Lindström, T.; Berglund, L.A.; Ikkala, O. Long and Entangled Native Cellulose I Nanofibers Allow Flexible Aerogels and Hierarchically Porous Templates for Functionalities. *Soft Matter* **2008**, *4*, 2492–2499. [CrossRef]

80. Sehaqui, H.; Salajková, M.; Zhou, Q.; Berglund, L.A. Mechanical Performance Tailoring of Tough Ultra-High Porosity Foams Prepared from Cellulose I Nanofiber Suspensions. *Soft Matter* **2010**, *6*, 1824–1832. [CrossRef]

81. Revin, V.V.; Pestov, N.A.; Shchankin, M.V.; Mishkin, V.P.; Platonov, V.I.; Uglanov, D.A. A Study of the Physical and Mechanical Properties of Aerogels Obtained from Bacterial Cellulose. *Biomacromolecules* **2019**, *20*, 1401–1411. [CrossRef] [PubMed]

82. Wu, Z.Y.; Li, C.; Liang, H.W.; Chen, J.F.; Yu, S.H. Ultralight, Flexible, and Fire-Resistant Carbon Nanofiber Aerogels from Bacterial Cellulose. *Angew. Chem. Int. Ed.* **2013**, *125*, 2997–3001. [CrossRef]

83. Yang, J.; Li, Y.; Zheng, Y.; Xu, Y.; Zheng, Z.; Chen, X.; Liu, W. Versatile Aerogels for Sensors. *Small* **2019**, *15*, 1902826. [CrossRef]

84. Kallmes, O.; Corte, H.H. The Structure of Paper, I. The Statistical Geometry of an Ideal Two Dimensional Fiber Network. *Tappi J.* **1960**, *43*, 737–752.

85. Baum, G.A. Orthotropic Elastic Constants of Paper. *Tappi J.* **1981**, *64*, 97–101.

86. Nissan, A.H. A Molecular Approach to the Problem of Viscoelasticity. *Nature* **1955**, *175*, 424. [CrossRef]

87. Nissan, A.H. H-Bond Dissociation in Hydrogen Bond Dominated Solids. *Macromolecules* **1976**, *9*, 840–850. [CrossRef]

88. Dufresne, A.; Cavaille, J.Y.; Vignon, M.R. Mechanical Behavior of Sheets Prepared from Sugar Beet Cellulose Microfibrils. *J. Appl. Polym. Sci.* **1997**, *64*, 1185–1194. [CrossRef]

89. Naghdi, T.; Yousefi, H.; Sharifi, A.R.; Golmohammadi, H. Nanopaper-Based Sensors. *Compr. Anal. Chem.* **2020**, *89*, 257–312.

90. Kontturi, E.; Tammelin, T.; Österberg, M. Cellulose—Model Films and the Fundamental Approach. *Chem. Soc. Rev.* **2006**, *35*, 1287–1304. [CrossRef]

91. Paunonen, S. Strength and Barrier Enhancements of Cellophane and Cellulose Derivative Films: A Review. *BioResources* **2013**, *8*, 3098–3121. [CrossRef]

92. Giese, M.; Blusch, L.K.; Khan, M.K.; Hamad, W.Y.; Maclachlan, M.J. Responsive Mesoporous Photonic Cellulose Films by Supramolecular Cotemplating. *Angew. Chem. Int. Ed.* **2014**, *126*, 9026–9030. [CrossRef]

93. Nogi, M.; Iwamoto, S.; Nakagaito, A.N.; Yano, H. Optically Transparent Nanofiber Paper. *Adv. Mater.* **2009**, *21*, 1595–1598. [CrossRef]

94. Benítez, A.J.; Torres-Rendon, J.; Poutanen, M.; Walther, A. Humidity and Multiscale Structure Govern Mechanical Properties and Deformation Modes in Films of Native Cellulose Nanofibrils. *Biomacromolecules* **2013**, *14*, 4497–4506. [CrossRef]

95. Hoeger, I.; Rojas, O.J.; Efimenko, K.; Velev, O.D.; Kelley, S.S. Ultrathin Film Coatings of Aligned Cellulose Nanocrystals from a Convective-Shear Assembly System and Their Surface Mechanical Properties. *Soft Matter* **2011**, *7*, 1957–1967. [CrossRef]

96. Zhao, T.H.; Parker, R.M.; Williams, C.A.; Lim, K.T.; Frka-Petesic, B.; Vignolini, S. Printing of Responsive Photonic Cellulose Nanocrystal Microfilm Arrays. *Adv. Funct. Mater.* **2019**, *29*, 1804531. [CrossRef]

97. Arcot, L.R.; Gröschel, A.H.; Linder, M.B.; Rojas, O.J.; Ikkala, O. Self-Assembly of Native Cellulose Nanostructures. In *Handbook of Nanocellulose and Cellulose Nanocomposites*; Wiley-VCH Verlag GmbH & Co., KGaA: Weinheim, Germany, 2017; Volume 1, pp. 123–174.

98. Zhang, J.; Elder, T.J.; Pu, Y.; Ragauskas, A.J. Facile Synthesis of Spherical Cellulose Nanoparticles. *Carbohydr. Polym.* **2007**, *69*, 607–611. [CrossRef]

99. Liebert, T.; Kostag, M.; Wotschadlo, J.; Heinze, T. Stable Cellulose Nanospheres for Cellular Uptake. *Macromol. Biosci.* **2011**, *11*, 1387–1392. [CrossRef]

100. Nikolajski, M.; Wotschadlo, J.; Clement, J.H.; Heinze, T. Amino-Functionalized Cellulose Nanoparticles: Preparation, Characterization, and Interactions with Living Cells. *Macromol. Biosci.* **2012**, *12*, 920–925. [CrossRef]

101. Beaumont, M.; Rosenfeldt, S.; Tardy, B.L.; Gusenbauer, C.; Khakalo, A.; Opietnik, M.; Potthast, A.; Rosenau, T. Synthesis of Redispersible Spherical Cellulose II Nanoparticles Decorated with Carboxylate Groups. *Green Chem.* **2016**, *18*, 1465–1468. [CrossRef]

102. Beaumont, M.; Rosenfeldt, S.; Tardy, B.L.; Gusenbauer, C.; Khakalo, A.; Nonappa, N.; Opietnik, M.; Potthast, A.; Rojas, O.J.; Rosenau, T. Soft Cellulose I$_I$ Nanospheres: Sol–Gel Behaviour, Swelling and Material Synthesis. *Nanoscale* **2019**, *11*, 17773–17781. [CrossRef]

103. Kulterer, M.R.; Reischl, M.; Reichel, V.E.; Hribernik, S.; Wu, M.; Köstler, S.; Kargl, R.; Ribitsch, V. Nanoprecipitation of Cellulose Acetate Using Solvent/Nonsolvent Mixtures as Dispersive Media. *Colloids Surf. A Physicochem. Eng. Asp.* **2011**, *375*, 23–29. [CrossRef]

104. Zhang, L.Q.; Niu, B.; Yang, S.G.; Huang, H.D.; Zhong, G.J.; Li, Z.M. Simultaneous Preparation and Dispersion of Regenerated Cellulose Nanoparticles Using a Facile Protocol of Dissolution–Gelation–Isolation–Melt Extrusion. *ACS Sustain. Chem. Eng.* **2016**, *4*, 2470–2478. [CrossRef]

105. Ioelovich, M. Nanoparticles of Amorphous Cellulose and Their Properties. *Am. J. Nanosci. Nanotech.* **2013**, *1*, 41–45. [CrossRef]

106. Beaumont, M.; Rennhofer, H.; Opietnik, M.; Lichtenegger, H.C.; Potthast, A.; Rosenau, T. Nanostructured Cellulose Ii Gel Consisting of Spherical Particles. *ACS Sustain. Chem. Eng.* **2016**, *4*, 4424–4432. [CrossRef]

107. Sharma, P.R.; Trimukhe, K.D.; Varma, A.J. Spherical Shaped Nanoparticles of Cellulose and Its Derivatives: A Short Review. *Trends Carbohyd. Res.* **2015**, *7*, 1–5.

108. Solin, K.; Beaumont, M.; Rosenfeldt, S.; Orelma, H.; Borghei, M.; Bacher, M.; Opietnik, M.; Rojas, O.J. Self-Assembly of Soft Cellulose Nanospheres into Colloidal Gel Layers with Enhanced Protein Adsorption Capability for Next-Generation Immunoassays. *Small* **2020**, *16*, 2004702. [CrossRef]

109. Lundahl, M.J.; Klar, V.; Wang, L.; Ago, M.; Rojas, O.J. Spinning of Cellulose Nanofibrils into Filaments: A Review. *Ind. Eng. Chem. Res.* **2017**, *56*, 8–19. [CrossRef]

110. Willberg-Keyriläinen, P.; Rokkonen, T.; Malm, T.; Harlin, A.; Ropponen, J. Melt Spinnability of Long Chain Cellulose Esters. *J. Appl. Polym. Sci.* **2020**, *137*, 49588. [CrossRef]

111. Frey, M.W. Electrospinning Cellulose and Cellulose Derivatives. *Polym. Rev.* **2008**, *48*, 378–391. [CrossRef]

112. Araki, J.; Miyayama, M. Wet Spinning of Cellulose Nanowhiskers; Fiber Yarns Obtained Only from Colloidal Cellulose Crystals. *Polymer* **2020**, *188*, 122116. [CrossRef]

113. Siró, I.; Plackett, D. Microfibrillated Cellulose and New Nanocomposite Materials: A Review. *Cellulose* **2010**, *17*, 459–494. [CrossRef]

114. Marques, P.A.; Nogueira, H.I.; Pinto, R.J.; Neto, C.P.; Trindade, T. Silver-Bacterial Cellulosic Sponges as Active Sers Substrates. *J. Raman Spectrosc.* **2008**, *39*, 439–443. [CrossRef]

115. Ogundare, S.A.; van Zyl, W.E. A Review of Cellulose-Based Substrates for Sers: Fundamentals, Design Principles, Applications. *Cellulose* **2019**, *26*, 6489–6528. [CrossRef]

116. Ranoszek-Soliwoda, K.; Tomaszewska, E.; Socha, E.; Krzyczmonik, P.; Ignaczak, A.; Orlowski, P.; Krzyzowska, M.; Celichowski, M.; Grobelny, J. The Role of Tannic Acid and Sodium Citrate in the Synthesis of Silver Nanoparticles. *J. Nanopart. Res.* **2017**, *19*, 1–15. [CrossRef]

117. Tran, C.D. Subnanogram Detection of Dyes on Filter Paper by Surface-Enhanced Raman Scattering Spectrometry. *Anal. Cham.* **1984**, *56*, 824–826.

118. Vo-Dinh, T.; Hiromoto, M.Y.K.; Begun, G.M.; Moody, R.L. Surface-Enhanced Raman Spectrometry for Trace Organic Analysis. *Anal. Cham.* **1984**, *56*, 1667–1670. [CrossRef]

119. Wei, W.; Huang, Q. Preparation of Cellophane-Based Substrate and Its Sers Performance on the Detection of Cv and Acetamiprid. *Spectrochim. Acta A Mol. Biomol. Spectrosc.* **2018**, *193*, 8–13. [CrossRef]

120. Kang, Y.; Kim, H.J.; Lee, S.H.; Noh, H. Paper-Based Substrate for a Surface-Enhanced Raman Spectroscopy Biosensing Platform—A Silver/Chitosan Nanocomposite Approach. *Biosensors* **2022**, *12*, 266. [CrossRef]

121. Morales-Narváez, E.; Golmohammadi, H.; Naghdi, T.; Yousefi, H.; Kostiv, U.; Horák, D.; Pourreza, N.; Merkoçi, A. Nanopaper as an Optical Sensing Platform. *ACS Nano* **2015**, *9*, 7296–72305. [CrossRef]

122. Park, M.; Chang, H.; Jeong, D.H.; Hyun, J. Spatial Deformation of Nanocellulose Hydrogel Enhances Sers. *BioChip J.* **2013**, *7*, 234–241. [CrossRef]

123. Wu, X.; Lu, C.; Zhang, W.; Yuan, G.; Xiong, R.; Zhang, X. A Novel Reagentless Approach for Synthesizing Cellulose Nanocrystal-Supported Palladium Nanoparticles with Enhanced Catalytic Performance. *J. Mater. Chem. A* **2013**, *1*, 8645–8652. [CrossRef]

124. Yan, W.; Chen, C.; Wang, L.; Zhang, D.; Li, A.J.; Yao, Z.; Shi, L.Y. Facile and Green Synthesis of Cellulose Nanocrystal-Supported Gold Nanoparticles with Superior Catalytic Activity. *Carbohydr. Polym.* **2016**, *140*, 66–73. [CrossRef]

125. Padalkar, S.; Capadona, J.R.; Rowan, S.J.; Weder, C.; Won, Y.H.; Stanciu, L.A.; Moon, R.J. Natural Biopolymers: Novel Templates for the Synthesis of Nanostructures. *Langmuir* **2010**, *26*, 8497–84502. [CrossRef]

126. Ifuku, S.; Tsuji, M.; Morimoto, M.; Saimoto, H.; Yano, H. Synthesis of Silver Nanoparticles Templated by Tempo-Mediated Oxidized Bacterial Cellulose Nanofibers. *Biomacromolecules* **2009**, *10*, 2714–2717. [CrossRef]

127. Rusin, C.J.; El Bakkari, M.; Du, R.; Boluk, Y.; McDermott, M.T. Plasmonic Cellulose Nanofibers as Water-Dispersible Surface-Enhanced Raman Scattering Substrates. *ACS Appl. Nano Mater.* **2020**, *3*, 6584–6597. [CrossRef]

128. Jiang, F.; Hsieh, Y.L. Synthesis of Cellulose Nanofibril Bound Silver Nanoprism for Surface Enhanced Raman Scattering. *Biomacromolecules* **2014**, *15*, 3608–3616. [CrossRef]

129. Nabeela, K.; Thomas, R.T.; Nair, J.B.; Maiti, K.K.; Warrier, K.G.K.; Pillai, S. Tempo-Oxidized Nanocellulose Fiber-Directed Stable Aqueous Suspension of Plasmonic Flower-Like Silver Nanoconstructs for Ultra-Trace Detection of Analytes. *ACS Appl. Mater. Interfaces* **2016**, *8*, 29242–29251. [CrossRef]

130. Wu, J.; Xi, J.; Chen, H.; Li, S.; Zhang, L.; Li, P.; Wu, W. Flexible 2d Nanocellulose-Based Sers Substrate for Pesticide Residue Detection. *Carbohydr. Polym.* **2022**, *277*, 118890. [CrossRef]

131. Li, M.; Li, X.; Xiao, H.N.; James, T.D. Fluorescence Sensing with Cellulose-Based Materials. *ChemistryOpen* **2017**, *6*, 685–696. [CrossRef]

132. Yang, Q.; Pan, X. A Facile Approach for Fabricating Fluorescent Cellulose. *J. Appl. Polym. Sci.* **2010**, *117*, 3639–3644. [CrossRef]

133. Sarrazin, P.; Valecce, L.; Beneventi, D.; Chaussy, D.; Vurth, L.; Stephan, O. Photoluminescent Paper Based on Poly(Fluorene-Co-Fluorenone) Particles Adsorption on Modified Cellulose Fibers. *Adv. Mater.* **2007**, *19*, 3291–3294. [CrossRef]

134. Nielsen, L.J.; Eyley, S.; Thielemans, W.; Aylott, J.W. Dual Fluorescent Labelling of Cellulose Nanocrystals for Ph Sensing. *Chem. Comm.* **2010**, *46*, 8929–8931. [CrossRef]

135. Helbert, W.; Chanzy, H.; Husum, T.L.; Schülein, M.; Ernst, S. Fluorescent Cellulose Microfibrils as Substrate for the Detection of Cellulase Activity. *Biomacromolecules* **2003**, *4*, 481–487. [CrossRef]

136. Wang, X.; Kim, Y.G.; Drew, C.; Ku, B.C.; Kumar, J.; Samuelson, L.A. Electrostatic Assembly of Conjugated Polymer Thin Layers on Electrospun Nanofibrous Membranes for Biosensors. *Nano Lett.* **2004**, *4*, 331–334. [CrossRef]

137. Davis, B.W.; Niamnont, N.; Hare, C.D.; Sukwattanasinitt, M.; Cheng, Q. Nanofibers Doped with Dendritic Fluorophores for Protein Detection. *ACS Appl. Mater. Interfaces* **2010**, *2*, 1798–1803. [CrossRef]

138. Fontenot, K.R.; Edwards, J.V.; Haldane, D.; Graves, E.; Citron, M.S.; Prevost, N.T.; Alfred, D.; French, A.D.; Condon, B.D. Human Neutrophil Elastase Detection with Fluorescent Peptide Sensors Conjugated to Cellulosic and Nanocellulosic Materials: Part Ii, Structure/Function Analysis. *Cellulose* **2016**, *23*, 1297–1309. [CrossRef]

139. Wang, M.; Meng, G.; Huang, Q.; Qian, Y. Electrospun 1,4-Dhaq-Doped Cellulose Nanofiber Films for Reusable Fluorescence Detection of Trace Cu^{2+} and Further for Cr^{3+}. *Environ. Sci. Technol.* **2012**, *46*, 367–373. [CrossRef]

140. Lu, W.; Zhang, J.; Huang, Y.; Théato, P.; Huang, Q.; Chen, T. Self-Diffusion Driven Ultrafast Detection of Ppm-Level Nitroaromatic Pollutants in Aqueous Media Using a Hydrophilic Fluorescent Paper Sensor. *ACS Appl. Mater. Interfaces* **2017**, *9*, 23884–23893. [CrossRef]

141. Ikai, T.; Suzuki, D.; Kojima, Y.; Yun, C.; Maeda, K.; Kanoh, S. Chiral Fluorescent Sensors Based on Cellulose Derivatives Bearing Terthienyl Pendants. *Polym. Chem.* **2016**, *7*, 4793–4801. [CrossRef]

142. Ikai, T.; Okamoto, Y. Structure Control of Polysaccharide Derivatives for Efficient Separation of Enantiomers by Chromatography. *Chem. Rev.* **2009**, *109*, 6077–6101. [CrossRef]

143. Sadollahkhani, A.; Hatamie, A.; Nur, O.; Willander, M.; Zargar, B.; Kazeminezhad, I. Colorimetric Disposable Paper Coated with Zno@Zns Core–Shell Nanoparticles for Detection of Copper Ions in Aqueous Solutions. *ACS Appl. Mater. Interfaces* **2014**, *6*, 17694–17701. [CrossRef]

144. Devarayan, K.; Kim, B.S. Reversible and Universal Ph Sensing Cellulose Nanofibers for Health Monitor. *Sens. Actuators B Chem.* **2015**, *209*, 281–286. [CrossRef]

145. Liang, T.; Sun, G.; Cao, L.; Li, J.; Wang, L. A pH and NH_3 Sensing Intelligent Film Based on Artemisia Sphaerocephala Krasch. Gum and Red Cabbage Anthocyanins Anchored by Carboxymethyl Cellulose Sodium Added as a Host Complex. *Food Hydrocoll.* **2019**, *87*, 858–868. [CrossRef]

146. Sheikhzadeh, E.; Naji-Tabasi, S.; Verdian, A.; Kolahi-Ahari, S. Equipment-Free and Visual Detection of Pb^{2+} Ion Based on Curcumin-Modified Bacterial Cellulose Nanofiber. *J. Iran. Chem. Soc.* **2021**, *19*, 283–290. [CrossRef]

147. Faham, S.; Ghavami, R.; Golmohammadi, H.; Khayatian, G. Spectrophotometric and Visual Determination of Zoledronic Acid by Using a Bacterial Cell-Derived Nanopaper Doped with Curcumin. *Microchim. Acta* **2019**, *186*, 719. [CrossRef] [PubMed]

148. Naghdi, T.; Golmohammadi, H.; Vosough, M.; Atashi, M.; Saeedi, I.; Maghsoudi, M.T. Lab-on-Nanopaper: An Optical Sensing Bioplatform Based on Curcumin Embedded in Bacterial Nanocellulose as an Albumin Assay Kit. *Anal. Chim. Acta* **2019**, *1070*, 104–111. [CrossRef] [PubMed]

149. Teodoro, K.B.; Migliorini, F.L.; Christinelli, W.A.; Correa, D.S. Detection of Hydrogen Peroxide (H_2O_2) Using a Colorimetric Sensor Based on Cellulose Nanowhiskers and Silver Nanoparticles. *Carbohydr. Polym.* **2019**, *212*, 235–241. [CrossRef] [PubMed]

150. Baretta, R.; Gabrielli, V.; Frasconi, M. Nanozyme–Cellulose Hydrogel Composites Enabling Cascade Catalysis for the Colorimetric Detection of Glucose. *ACS Appl. Nano Mater.* **2022**. [CrossRef]

151. Mahapatra, S.; Srivastava, V.R.; Chandra, P. Nanobioengineered Sensing Technologies Based on Cellulose Matrices for Detection of Small Molecules, Macromolecules, and Cells. *Biosensors* **2021**, *11*, 168.

152. Lawrence, C.S.K.; Tan, S.N.; Floresca, C.Z. A "Green" Cellulose Paper Based Glucose Amperometric Biosensor. *Sens. Actuators B Chem.* **2014**, *193*, 536–541. [CrossRef]

153. Koga, H.; Kitaoka, T.; Isogai, A. Paper-Immobilized Enzyme as a Green Microstructured Catalyst. *J. Mater. Chem.* **2012**, *12*, 11591–11597. [CrossRef]

154. Sun, B.; Wang, Z.; Wang, X.; Qiu, M.; Zhang, Z.; Wang, Z.; Cui, J.; Jia, S. Paper-Based Biosensor Based on Phenylalnine Ammonia Lyase Hybrid Nanoflowers for Urinary Phenylalanine Measurement. *Int. J. Biol. Macromol.* **2021**, *166*, 601–610. [CrossRef]

155. Bumbudsanpharoke, N.; Kwon, S.; Lee, W.; Ko, S. Optical Response of Photonic Cellulose Nanocrystal Film for a Novel Humidity Indicator. *Intern. J. Biol. Macromol.* **2019**, *140*, 91–97. [CrossRef]

156. Dai, S.; Prempeh, N.; Liu, D.; Fan, Y.; Gu, M.; Chang, Y. Cholesteric Film of Cu(Ii)-Doped Cellulose Nanocrystals for Colorimetric Sensing of Ammonia Gas. *Carbohydr. Polym.* **2017**, *174*, 531–539. [CrossRef]

157. Song, W.; Lee, J.K.; Gong, M.S.; Heo, K.; Chung, W.J.; Lee, B.Y. Cellulose Nanocrystal-Based Colored Thin Films for Colorimetric Detection of Aldehyde Gases. *ACS Appl. Mater. Interfaces* **2018**, *10*, 10353–10361. [CrossRef] [PubMed]

158. Kose, O.; Tran, A.; Lewis, L.; Hamad, W.Y.; MacLachlan, M.J. Unwinding a Spiral of Cellulose Nanocrystals for Stimuli-Responsive Stretchable Optics. *Nat. Commun.* **2019**, *10*, 510. [CrossRef]

159. Mansfield, M.A. Nitrocellulose Membranes for Lateral Flow Immunoassays: A Technical Treatise. In *Lateral Flow Immunoassay*; Human Press: New York, NY, USA, 2009; pp. 1–19.

160. Lappalainen, T.; Vento, P.; Teerinen, T.; Erho, T.; Hakalahti, L. Cellulose as a Novel Substrate for Lateral Flow Assay. *Nordic Pulp Paper Res. J.* **2010**, *25*, 536–550. [CrossRef]

161. Teerinen, T.; Lappalainen, T.; Erho, T. A Paper-Based Lateral Flow Assay for Morphine. *Anal. Bioanal. Chem.* **2014**, *406*, 5955–5965. [CrossRef]

162. Quesada-González, D.; Stefani, C.; González, I.; De La Escosura-Muñiz, A.; Domingo, N.; Mutjé, P.; Merkoçi, A. Signal Enhancement on Gold Nanoparticle-Based Lateral Flow Tests Using Cellulose Nanofibers. *Biosens. Bioelectron.* **2019**, *141*, 111407. [CrossRef]

163. Satheesh, N.; Jayaraj, J.; Prazeres, D.M.F. A Cellulose Paper-Based Fluorescent Lateral Flow Immunoassay for the Quantitative Detection of Cardiac Troponin, I. *Biosensors* **2021**, *11*, 49.

164. Frasconi, M.; Mazzarino, M.; Botrè, F.; Mazzei, F. Surface Plasmon Resonance Immunosensor for Cortisol and Cortisone Determination. *Anal. Bioanal. Chem.* **2009**, *394*, 2151–2159. [CrossRef]

165. Silin, V.; Weetall, H.; Vanderah, D.J. SPR Studies of the Nonspecific Adsorption Kinetics of Human Igg and BSA on Gold Surfaces Modified by Self-Assembled Monolayers (Sams). *J. Colloid. Interface Sci.* **1997**, *185*, 94–103. [CrossRef]

166. Culica, M.E.; Chibac-Scutaru, A.L.; Mohan, T.; Coseri, S. Cellulose-Based Biogenic Supports, Remarkably Friendly Biomaterials for Proteins and Biomolecules. *Biosens. Bioelectron.* **2021**, *182*, 113170. [CrossRef]

167. Miura, T.; Horiuchi, T.; Iwasaki, Y.; Seyama, M.; Camou, S.; Takahashi, J.I.; Haga, T. Patterned Cellulose Membrane for Surface Plasmon Resonance Measurement. *Sens. Actuators B Chem.* **2012**, *173*, 354–360. [CrossRef]

168. Berlin, P.; Klemm, D.; Jung, A.; Liebegott, H.; Rieseler, R.; Tiller, J. Film-Forming Aminocellulose Derivatives as Enzyme-Compatible Support Matrices for Biosensor Developments. *Cellulose* **2003**, *10*, 343–367. [CrossRef]

169. Tiller, J.; Klemm, D.; Berlin, P. Designed Aliphatic Aminocellulose Derivatives as Transparent and Functionalized Coatings for Enzyme Immobilization. *Des. Monomers Polym.* **2001**, *4*, 315–328. [CrossRef]

170. Tiller, J.C.; Rieseler, R.; Berlin, P.; Klemm, D. Stabilization of Activity of Oxidoreductases by Their Immobilization onto Special Functionalized Glass and Novel Aminocellulose Film Using Different Coupling Reagents. *Biomacromolecules* **2002**, *3*, 1021–1029. [CrossRef]

171. Ferreira, N.S.; Sales, M.G.F. Disposable Immunosensor Using a Simple Method for Oriented Antibody Immobilization for Label-Free Real-Time Detection of an Oxidative Stress Biomarker Implicated in Cancer Diseases. *Biosens. Bioelectron.* **2014**, *53*, 193–199. [CrossRef]

172. Juan-Colás, J.; Johnson, S.; Krauss, T.F. Dual-Mode Electro-Optical Techniques for Biosensing Applications: A Review. *Sensors* **2017**, *17*, 2047. [CrossRef]

173. Migliorini, F.L.; Teodoro, K.B.; Scagion, V.P.; dos Santos, D.M.; Fonseca, F.J.; Mattoso, L.H.; Correa, D.S. Tuning the Electrical Properties of Electrospun Nanofibers with Hybrid Nanomaterials for Detecting Isoborneol in Water Using an Electronic Tongue. *Surfaces* **2019**, *2*, 432–443. [CrossRef]

174. Kumar, S.; Pandey, C.M.; Hatamie, A.; Simchi, A.; Willander, M.; Malhotra, B.D. Nanomaterial-Modified Conducting Paper: Fabrication, Properties, and Emerging Biomedical Applications. *Global Chall.* **2019**, *3*, 1900041. [CrossRef]

175. Chen, D.; Zhao, X.; Wei, X.; Zhang, J.; Wang, D.; Lu, H.; Jia, P. Ultrastretchable, Tough, Antifreezing, and Conductive Cellulose Hydrogel for Wearable Strain Sensor. *ACS Appl. Mater. Interfaces* **2020**, *12*, 53247–53256.

176. Chen, S.; Song, Y.; Ding, D.; Ling, Z.; Xu, F. Flexible and Anisotropic Strain Sensor Based on Carbonized Crepe Paper with Aligned Cellulose Fibers. *Adv. Funct. Mater.* **2018**, *28*, 1802547. [CrossRef]

177. Wang, M.; Anoshkin, I.V.; Nasibulin, A.G.; Korhonen, J.T.; Seitsonen, J.; Pere, J.; Kauppinen, E.I.; Ras, R.H.A.; Ikkala, O. Modifying Native Nanocellulose Aerogels with Carbon Nanotubes for Mechanoresponsive Conductivity and Pressure Sensing. *Adv. Mater.* **2013**, *25*, 2428–2432. [CrossRef]

178. Sadasivuni, K.K.; Kafy, A.; Zhai, L.; Ko, H.U.; Mun, S.; Kim, J. Transparent and Flexible Cellulose Nanocrystal/Reduced Graphene Oxide Film for Proximity Sensing. *Small* **2015**, *11*, 994–1002. [CrossRef]

179. Wang, J.; Golden, T.; Li, R. Cobalt Phthalocyanine Cellulose-Acetate Chemically Modified Electrodes for Electrochemical Detection in Flowing Streams—Multifunctional Operation Based Upon the Coupling of Electrocatalysis and Permselectivity. *Anal. Chem.* **1988**, *60*, 1642–1645. [CrossRef]

180. Wang, J.; Tuzhi, P. Selectivity and Sensitivity Improvements at Perfluorinated Ionomer/Cellulose Acetate Bilayer Electrodes. *Anal. Chem.* **1988**, *58*, 3257–3261. [CrossRef]

181. Wang, J.; Hutchins-Kumar, L.D. Cellulose Acetate Coated Mercury Film Electrodes for Anodic Stripping Voltammetry. *Anal. Cham.* **1986**, *58*, 402–407. [CrossRef]

182. Wang, J.; Hutchins, L.D. Thin-Layer Electrochemical Detector with a Glassy-Carbon Electrode Coated with a Base-Hydrolyzed Cellulosic Film. *Anal. Chem.* **1985**, *57*, 1536–1541. [CrossRef]

183. Hussin, H.; Gan, S.N.; Phang, S.W. Effect of Functional Groups in the Pani-Cellulose Derivatives-Based Sensor in Hydrazine Detection. *Polym. Bull.* **2021**, *79*, 1843–1856. [CrossRef]

184. Yang, L.; Xu, X.; Liu, M.; Chen, C.; Cui, J.; Chen, X.; Wu, K.; Sun, D. Wearable and Flexible Bacterial Cellulose/Polyaniline Ammonia Sensor Based on a Synergistic Doping Strategy. *Sens. Actuators B Chem.* **2021**, *334*, 129647. [CrossRef]

185. Chen, G.; Chen, T.; Hou, K.; Ma, W.; Tebyetekerwa, M.; Cheng, Y.; Weng, W.; Zhu, M. Robust, Hydrophilic Graphene/Cellulose Nanocrystal Fiber-Based Electrode with High Capacitive Performance and Conductivity. *Carbon* **2018**, *127*, 218–227. [CrossRef]

186. El Miri, N.; El Achaby, M.; Fihri, A.; Larzek, M.; Zahouily, M.; Abdelouahdi, K.; Barakat, A.; Solhy, A. Synergistic Effect of Cellulose Nanocrystals/Graphene Oxide Nanosheets as Functional Hybrid Nanofiller for Enhancing Properties of PVA Nanocomposites. *Carbohydr. Polym.* **2016**, *137*, 239–248. [CrossRef]

187. Koga, H.; Saito, T.; Kitaoka, T.; Nogi, M.; Suganuma, K.; Isogai, A. Transparent, Conductive, and Printable Composites Consisting of Tempo-Oxidized Nanocellulose and Carbon Nanotube. *Biomacromolecules* **2013**, *14*, 1160–1165. [CrossRef]

188. Durairaj, V.; Li, P.; Liljeström, T.; Wester, N.; Etula, J.; Leppänen, I.; Ge, Y.; Kontturi, K.S.; Tammelin, T.; Laurila, T.; et al. Functionalized Nanocellulose/Multiwalled Carbon Nanotube Composites for Electrochemical Applications. *ACS Appl. Nano Mater.* **2021**, *4*, 5842–5853. [CrossRef]

189. Morimune-Moriya, S.; Salajkova, M.; Zhou, Q.; Nishino, T.; Berglund, L.A. Reinforcement Effects from Nanodiamond in Cellulose Nanofibril Films. *Biomacromolecules* **2018**, *19*, 2423–2431. [CrossRef]

190. Durairaj, V.; Wester, N.; Etula, J.; Laurila, T.; Lehtonen, J.; Rojas, O.J.; Pahimanolis, N.; Koskinen, J. Multiwalled Carbon Nanotubes/Nanofibrillar Cellulose/Nafion Composite-Modified Tetrahedral Amorphous Carbon Electrodes for Selective Dopamine Detection. *J. Phys. Chem. C* **2019**, *123*, 24826–24836. [CrossRef]

191. Shalauddin, M.; Akhter, S.; Basirun, W.J.; Bagheri, S.; Anuar, N.S.; Johan, M.R. Hybrid Nanocellulose/F-Mwcnts Nanocomposite for the Electrochemical Sensing of Diclofenac Sodium in Pharmaceutical Drugs and Biological Fluids. *Electrochim. Acta* **2019**, *304*, 323–333. [CrossRef]

192. Ortolani, T.S.; Pereira, T.S.; Assumpç, M.H.M.T.; Vicentini, F.C.; de Oliveira, G.G.; Janegitz, B.C. Electrochemical Sensing of Purines Guanine and Adenine Using Single-Walled Carbon Nanohorns and Nanocellulose. *Electrochim. Acta* **2019**, *298*, 893–900. [CrossRef]

193. Liu, X.; Li, X.; Gao, X.; Ge, L.; Sun, X.; Li, F. A Universal Paper-Based Electrochemical Sensor for Zero-Background Assay of Diverse Biomarkers. *ACS Appl. Mater. Interfaces* **2019**, *11*, 15381–15388. [CrossRef]

194. Wang, C.; Wu, R.; Ling, H.; Zhao, Z.; Han, W.; Shi, X.; Payne, G.F.; Wang, X. Toward Scalable Fabrication of Electrochemical Paper Sensor without Surface Functionalization. *NPJ Flex. Electron.* **2022**, *6*, 12. [CrossRef]

195. Bi, Q.; Dong, S.; Sun, Y.; Lu, X.; Zhao, L. An Electrochemical Sensor Based on Cellulose Nanocrystal for the Enantioselective Discrimination of Chiral Amino Acids. *Anal. Biochem.* **2016**, *508*, 50–57. [CrossRef]

196. Mun, S.; Zhai, L.; Min, S.K.; Yun, Y.; Kim, J. Flexible and Transparent Strain Sensor Made with Silver Nanowire–Coated Cellulose. *J. Intell. Mater. Syst. Struct.* **2016**, *27*, 1011–1018. [CrossRef]

197. De, S.; Higgins, T.M.; Lyons, P.E.; Doherty, E.M.; Nirmalraj, P.N.; Blau, W.J.; Boland, J.J.; Coleman, J.N. Silver Nanowire Networks as Flexible, Transparent, Conducting Films: Extremely High Dc to Optical Conductivity Ratios. *ACS Nano* **2009**, *3*, 1767–1774. [CrossRef]

198. Zhai, L.; Kim, H.C.; Muthoka, R.M.; Latif, M.; Alrobei, H.; Malik, R.A.; Kim, J. Environment-Friendly Zinc Oxide Nanorods-Grown Cellulose Nanofiber Nanocomposite and Its Electromechanical and Uv Sensing Behaviors. *Nanomaterials* **2021**, *11*, 1419. [CrossRef]
199. Eynaki, H.; Kiani, M.A.; Golmohammadi, H. Nanopaper-Based Screen-Printed Electrodes: A Hybrid Sensing Bioplatform for Dual Opto-Electrochemical Sensing Applications. *Nanoscale* **2020**, *12*, 18409–18417. [CrossRef]